Atmos. Chem. Phys. Discuss., 11, 30665–30718, 2011
www.atmos-chem-phys-discuss.net/11/30665/2011/
doi:10.5194/acpd-11-30665-2011

Atmospheric Chemistry and Physics Discussions

Airborne measurements of trace gases and aerosols over the London metropolitan region

G. R. McMeeking[1,*], M. Bart[2], P. Chazette[3], J. M. Haywood[4,5], J. R. Hopkins[6], J. B. McQuaid[2], W. T. Morgan[1], J.-C. Raut[7], C. L. Ryder[8], N. Savage[4], K. Turnbull[4], and H. Coe[1]

[1]Centre for Atmospheric Science, University of Manchester, Manchester, UK
[2]School of Earth and Environment, University of Leeds, Leeds, UK
[3]Laboratoire des Sciences du Climat et de l'Environnement, Laboratoire mixte CEA-CNRS-UVSQ, CEA Saclay, Gif-sur-Yvette, France
[4]Observation Based Research, Met Office, Exeter, UK
[5]College of Engineering, Mathematics and Physical Sciences, University of Exeter, Exeter, UK
[6]Department of Chemistry, University of York, York, UK
[7]Laboratoire Atmosphères, Milieux et Observations Spatiales, Laboratoire mixte CNRS-UVSQ-UPMC, Université Paris, Paris, France

[8]Department of Meteorology, University of Reading, Reading, UK
[*]now at: Department of Atmospheric Science, Colorado State University, Fort Collins, CO, USA

Received: 21 October 2011 – Accepted: 31 October 2011 – Published: 16 November 2011

Correspondence to: G. R. McMeeking (gavin@atmos.colostate.edu)

Published by Copernicus Publications on behalf of the European Geosciences Union.

ACPD
11, 30665–30718, 2011

Abstract

The Emissions around the M25 motorway (EM25) campaign took place over the megacity of London in the United Kingdom in June 2009 with the aim of characterising trace gas and aerosol composition and properties entering and emitted from the urban region. It featured two mobile platforms, the UK BAe-146 Facility for Airborne Atmospheric Measurements (FAAM) research aircraft and a ground-based mobile lidar van, both travelling in circuits around London, roughly following the path of the M25 motorway circling the city. We present an overview of findings from the project, which took place during typical UK summertime pollution conditions. Emission ratios of volatile organic compounds (VOCs) emitted from the London region were consistent with measurements in and downwind of other large urban areas and indicated traffic and associated fuel evaporation were major sources. Sub-micron aerosol composition was dominated by secondary species including sulphate (24 % of sub-micron mass in the London plume and 30 % in the background aerosol), nitrate (24 % plume; 18 % background) and organic aerosol (30 % plume; 30 % background). The primary sub-micron aerosol emissions from London were minor compared to the larger regional background, with only limited increases in aerosol mass in the urban plume compared to the background (15 % mass increase on average). Black carbon mass was the major exception, which more than doubled in the urban plume and lead to a decrease in the single scattering albedo from 0.91 in the background aerosol to 0.86 in the London plume, on average. Our observations indicated that regional aerosol appeared to dominate urban sources, at least during typical summertime conditions, meaning future efforts to reduce PM levels in London must account for regional as well as local aerosol sources.

ACPD

11, 30665–30718, 2011

1 Introduction

The greater London urban region is home to approximately 8–12 million people, making it the largest conurbation in the United Kingdom and one of a growing number of megacities throughout the world. Globally, over half of the world's human population lives in urban areas, many of them megacities, and these numbers are expected to grow in the coming years. Megacities frequently have very high concentrations of observed air pollutants (Banta et al., 2005), which combined with their large populations results in serious health and visibility impacts (Garland et al., 2008; Parekh, 2001). In addition to local impacts, the large emissions of pollutants from megacities make them important contributors to air pollution on regional and global scales (Lawrence et al., 2007; Molina and Molina, 2004). Cities emit primary aerosols as well as oxides of nitrogen (NO_x) and volatile organic compounds (VOCs) that drive photochemical smog formation and also oxidise to secondary aerosol precursors.

The importance of megacity emissions has motivated several recent studies featuring a combination of measurements and numerical modelling to examine aerosol and trace gas emissions and atmospheric processing. These include the MILAGRO (Megacity Initiative: Local and Global Research Observations) (Molina et al., 2010) Mexico City case study in 2006 and the CalNex (Research at the Nexus of Air Quality and Climate Change) intensive measurement period in Los Angeles in 2010. In Europe, components of the MEGAPOLI (Megacities: emissions, urban, regional and Global Atmospheric POLlution and climate effects, and Integrated tools for assessment and mitigation) project examined emissions from Paris, France in 2009 and 2010. It followed the original experiments conducted within the frame of the Etude et Simulation de la Qualité de l'air en region Ile-de-France (ESQUIF) program (Chazette et al., 2005; Menut et al., 2000). Results from these recent campaigns have underscored the importance of oxygenated organic and secondary inorganic aerosol species to PM concentrations even in major urban locations (e.g., Aiken et al., 2009).

ACPD
11, 30665–30718, 2011

In London, the introduction of air quality control strategies going back to at least the early 1990s has led to reductions in gas- and particle-phase pollutants (Bigi and Harrison, 2010). Some species, including ozone (Bigi and Harrison, 2010), have increased, while recent trends in $PM_{2.5}$ and PM_{10} (particulate matter with aerodynamic diameters <2.5 µm and 10 µm, respectively) concentrations have remained flat or even increased, despite predicted reductions from emissions inventories (Fuller and Green, 2006). Further reductions in PM have proved elusive. For example, the contribution from road transport was expected to decrease following the introduction of a number of control strategies, including the inner London congestion charge scheme, however the impacts of the scheme and other control strategies on surface pollutant concentrations have been mixed (Atkinson et al., 2009). The upcoming 2012 London Olympics has also drawn more attention to air quality in the London region and its potential effects on the games.

Previous measurements have provided valuable information regarding the chemical make-up and sources of PM in London, but did not provide a characterisation of background aerosol upwind of London nor described how London emissions affect aerosol properties downwind of the city. Additional measurements of aerosol chemical composition in London are needed to improve both our understanding of current trends in monitoring observations and to improve emission inventories. Better understanding of the contributions from nitrate, sulphate and secondary organic aerosol (SOA) to regional background aerosol concentrations is also needed. Motivated by these needs, the EM25 (EMissions around the M25) project focused on aircraft-based in situ observations of aerosols and trace gases and remotely sensed aerosol properties measured by a ground-based mobile lidar up- and downwind of Greater London. The mobile platforms travelled in circuits roughly encompassing the M25 motorway "ring road", shown in Fig. 1a. This approach allowed us to sample air upwind and downwind of London and compare the urban emissions with regional pollution moving over the city. Here we present an overview of major findings from the campaign to serve as a background for more detailed analyses of trace gas and aerosol properties.

ACPD
11, 30665–30718, 2011

London is located in south-eastern England in the United Kingdom (Fig. 1a) and has essentially a maritime climate. The major contributors to emissions in London depend on pollutant type. Road transport (52 % of total emissions including passenger cars, 17 %, and rigid heavy-duty vehicles, 13 %) and natural gas use (32 %) were the most important source types of nitrogen oxides (NO_x) within the M25 in 2004 according to the London Atmospheric Emissions Inventory (LAEI; Mattai and Hutchinson, 2008). Major VOC emission sources in the London region include the evaporation of industrial solvents and petrol (45 % total VOC emissions), road transport (30 %), and agricultural or natural sources including urban parks (20 %). The main contributors to the sources of particulate matter in London are road traffic (producing primary aerosol from both exhaust and non-exhaust emissions), primary particles from industry, and secondary particles from the oxidation of SO_2, NO_x and VOCs emitted by traffic and industry (Harrison et al., 2004). Transport of regional PM, such as aged organic aerosol, also contributes to London aerosol mass concentrations in addition to the local sources (Allan et al., 2010).

2 Methods

The EM25 campaign took place between 16–24 June 2009 in and around the Greater London region. In addition to a number of gas and aerosol long-term monitoring sites, the experiment featured two mobile measurement platforms, the UK Facility for Airborne Atmospheric Measurements (FAAM) modified BAe-146 research aircraft and a van fitted with a mobile lidar system, both described in detail below. The FAAM research aircraft flight tracks were designed to follow the M25 motorway as closely as possible at a minimum safe altitude of ~750 m above ground level (a.g.l.), but deviated in the western and southern portions of the circuit to comply with air traffic control restrictions owing to the proximity of the Heathrow and Gatwick terminal manoeuvring areas. Vertical profiles were obtained during each flight by flying "missed approaches" into Northolt, Farnborough, and Southport airfields (Fig. 1), selected based on the

ACPD
11, 30665–30718, 2011

prevailing wind direction to probe the atmosphere to ~20 m a.g.l. The research flights and lidar van deployments were coordinated to allow simultaneous sampling for the dates listed in Table 1.

2.1 FAAM research aircraft and instruments

The FAAM research aircraft is a BAe-146 jet modified for atmospheric measurements and has participated in a large number of campaigns since 2004. Real-time measurements of carbon monoxide, nitrogen oxides and ozone were made by an Aero-Laser AL5002 VUV resonance fluorescence gas analyser, a chemiluminescence gas analyser (Thermo Scientific Model 42) and a UV photometric gas analyser (Thermo Environmental Instruments Inc., USA, Model 49C), respectively. Calibration procedures for the real-time gas analysers are described by Hopkins et al. (2006). Whole air canister samples were collected in 3 l silica coated stainless steel canisters (Thames Restek, UK) using an all-stainless steel assembly double headed bellows pump (Senior Aerospace, USA), which drew air from the main sampling manifold of the aircraft and pressurised air into canisters to a maximum pressure of ~3 bar. Samples were usually collected over approximately one minute intervals during selected portions of each flight. The samples were analysed off-line for VOCs using a dual channel gas chromatograph with flame ionisation detection (Hopkins et al., 2011).

Aerosol composition measurements were made by an Aerodyne compact Time-of-Flight Aerosol Mass Spectrometer (cToF-AMS) (Canagaratna et al., 2007; Drewnick et al., 2005; Morgan et al., 2010a) and a DMT Single Particle Soot Photometer (SP2) (Baumgardner et al., 2004; McMeeking et al., 2010; Schwarz et al., 2006). The AMS provided size-resolved chemical composition information for sub-micron, non-refractory particulate matter, classified as organic aerosol (OA), sulphate, nitrate, ammonium and non-sea salt chloride. The SP2 made size-resolved measurements of refractory black carbon (rBC) mass for "cores" between approximately 0.5–300 fg and also provided information regarding the rBC mixing state for a subset of the measured particles (Moteki and Kondo, 2007). The AMS was calibrated and data were

ACPD
11, 30665–30718, 2011

analysed following the procedures described in detail by Morgan et al. (2010b). The SP2 data analysis followed the procedures described by McMeeking et al. (2010) and calibrations were performed using mobility diameter-selected glassy carbon spheres and polystyrene latex spheres (PSL).

Aerosol number distributions were measured by a wing-mounted passive cavity aerosol spectrometer probe (PCASP-100X with SPP-200 hardware upgrade), which optically counted and sized particles between 0.1 and 3 µm diameter. Particle size bins up to 0.8 µm were calibrated using ammonium sulphate, which was converted to a PSL-equivalent diameter using Mie theory. Coarse mode aerosol and cloud hydrometeors in the size range 0.5–50 µm diameter were counted and sized using a DMT cloud aerosol spectrometer (CAS) operating as part of a wing-mounted DMT cloud, aerosol and precipitation spectrometer (CAPS) probe. Daily checks of the CAS size calibration were performed using glass beads. Aerosol number concentrations (diameter > 3 nm) were measured by a modified TSI 3786 ultrafine water-based condensation particle counter (WCPC).

Wet and dry aerosol light scattering (b_{sp}) and ambient absorption (b_{ap}) coefficients were measured by two TSI 3563 integrating nephelometers (Haywood et al., 2008a) and a particle soot absorption photometer (PSAP). The dry and wet nephelometer measurements were corrected for angular truncation and non-Lambertian light-source errors using the sub-micron correction parameters provided by Anderson and Ogren (1998). The nephelometer system performed scans between 40–90 % relative humidity (RH) to determine the light scattering growth factor or f(RH) (Morgan et al., 2010a). The average scan cycle (up and down) took between 10–30 min to complete. The PSAP measurements were corrected following Bond et al. (1999) to account for variations in the particle deposit spot size, instrument flow rate and adjust the measurement to 550 nm wavelength for comparing with the 550 nm nephelometer wavelength.

All on-board aerosol instruments sampled ambient air via stainless steel tubing through Rosemount inlets. The inlet efficiency for super-micron particles is believed to be low (Haywood et al., 2003), so the aircraft measurements are thought to represent

ACPD
11, 30665–30718, 2011

predominantly sub-micron aerosol properties. Aerosol number and mass concentrations, scattering and absorption coefficients are reported at standard temperature and pressure (STP) defined as 273.15 K and 1013.25 hPa. For clarity, these parameters are denoted using an "s" (e.g., sm^3) to distinguish them from ambient concentrations and coefficients. All real-time measurements were averaged to the approximately 30 s time resolution of the AMS or the sampling interval of the whole air canister samplers, if collected. Table 2 summarizes the instruments involved in the project.

2.2 Ground-based mobile LIDAR

The Aerosol Lidar System (ALS) is a custom-built backscatter lidar emitting in the ultraviolet developed by the Commissariat à l'Energie Atomique (CEA) and the Centre National de la Recherche Scientifique (CNRS) (Chazette et al., 2007). It is now available commercially from the LEOSPHERE Company under the name of EZ Lidar® (www.leosphere.com). It is designed to monitor the aerosol dispersion in the low and middle troposphere and operated with a Nd:YAG laser at the wavelength of 355 nm. The detection system had parallel and cross-polarised detection channels. The resolution along the line of sight was 1.5 m and had an overlap factor close to 1 at ~150 m a.g.l. The advantages of operating the lidar from a small vehicle were that it was able to follow small atmospheric features (Raut and Chazette, 2009; Royer et al., 2011) and could examine the role of the M25 traffic in the production of anthropogenic aerosols. The lidar signals have been calibrated, corrected from the background sky radiance and range-corrected.

2.3 Ground-based fixed measurements

In addition to the aircraft and ground-based lidar measurements, we used three networks of ground-based measurements across London to provide information on aerosol distribution within the circuits performed by the mobile measurements. The first was a well-established network of air quality measurements run by the London Air

ACPD
11, 30665–30718, 2011

Quality Network (http://www.londonair.org.uk) (Atkinson et al., 2009; Fuller and Green, 2006), which includes measurements of PM_{10} concentrations at most stations, and $PM_{2.5}$ at a subset of these measured with a Tapered Element Oscillating Microbalance (see Fig. 1a). The stations represent a variety of site types, including suburban, urban background, industrial, roadside and kerbside locations. Second, we analysed data from a new network of weather stations which was set up as part of the OPen Air Laboratories (OPAL) project (Davies et al., 2011). The weather stations are Davis Vantage Pro2 Plus automatic weather stations measuring standard meteorological variables, although during EM25 measurements of solar irradiance were used to infer column aerosol loadings on clear days (Ryder and Toumi, 2011). The third network included two locations that are part of the UK Automated Hydrocarbon Network, a kerb-side site (Marylebone Road) and a suburban site (Eltham). Both sites feature automatic Perkin Elmer gas chromatograph systems measuring over 25 different hydrocarbon species.

3 Results and discussion

3.1 Meteorology and transport

Flight operations during the June 2009 EM25 campaign window targeted polluted conditions to assess pollution transport into and out of the London region. Meteorological conditions during the five flight days are summarized in Fig. 2, which shows the 850 hPa geopotential height fields and 850 hPa pressure level winds from the ECMWF ERA Interim re-analysis. The first two flights on 16 and 18 June took place before and after the passage of a precipitating cold front over the UK. The 850 hPa pressure-level winds on 16 June over the London region were light and variable, though generally westerly or southwesterly, changing to westerly on 18 June following the passage of a front the previous night. The final three flights took place between 22–24 June, when a high pressure system moved eastwards from southern Ireland to southern Norway. Flow over the London region changed from light northerlies on 22 June to easterlies on

ACPD
11, 30665–30718, 2011

23–24 June. There were usually scattered fair weather cumulus clouds over the study region with no precipitation on flight days, though cloud base was above the flight measurement altitude for all but a few brief periods, which have been removed from the analysis.

We examined aerosol mass concentrations measured by the ground stations to provide context for the aircraft measurements during the EM25 campaign. Fig. 3 shows $PM_{2.5}$ and PM_{10} concentrations from the London ground stations shown in Fig. 1a with summertime (June/July) mean values for the period 2005–2009. Mass concentrations were near or slightly below their July/July 2005–2009 averages (approximately 15 $\mu g\,m^{-3}$) from 16 June to 22 June. $PM_{2.5}$ concentrations then increased to above average (20 $\mu g\,m^{-3}$), reflecting the change from predominantly westerly to easterly winds and associated transport of pollution from continental Europe (Bigi and Harrison, 2010).

Forecast aerosol mass concentrations from the 4 km resolution operational numerical weather prediction (NWP) model (Clark et al., 2008; Haywood et al., 2008b) showed transport patterns and expected pollution "hotspots" in the London area. In addition to providing standard meteorological variables such as temperature, humidity, cloud and precipitation fields, the UK4 model included a highly simplified representation of aerosol emission, transformation, and deposition (Clark et al., 2008). Sources of aerosol were based on the European emission inventory on a 1/8 degree by 1/16 degree grid developed for the GEMS project by Visschedijk et al. (2007) plus ship emissions from the European Monitoring and Evaluation Programme (EMEP) emissions database for 2005. The aerosol was represented by a single tracer (generically termed "murk") which approximately accounted for sources from SO_2, NO_x and VOCs by using a factor representing the average conversion of the gas emissions to aerosol within the model domain. The emission fields used by the model are shown in Fig. 1b. The aerosol concentration was used along with a mean hygroscopic growth factor to provide forecasts of atmospheric visibility (Haywood et al., 2008b). The hygroscopic growth factor used was based on nephelometer data from previous flight campaigns.

ACPD
11, 30665–30718, 2011

Variational data-assimilation of observed visibilities were used to correct the model fields of aerosol mass concentration and relative humidity (Clark et al., 2008).

Snapshots of the predicted aerosol mass distribution are shown in Fig. 4 for illustrative purposes timed at approximately the middle of aircraft circuits. At the 760 m model level nearest to the aircraft altitude during circuits, the highest aerosol emissions were predicted to be around London. The predicted plume advected southeast and east for the northwesterly and westerly flights (16 and 18 June; Fig. 4a and b), west for the two easterly flow cases (23 and 24 June; Fig. 4d and e) and remained over the London region and slightly to the north for the stagnant 22 June flight (Fig. 4c). Plumes from the Southampton area to the southwest of London may have reached the flight track for the 16 and 18 June flights. The visibility model also showed emissions from the coal-fired Didcot power station (shown in Fig. 1a) possibly reaching the flight track on 16, 22 and 23 June. The model predicted the highest and lowest aerosol concentrations over London on 22 and 18 June, respectively.

3.2 Trace gas measurements

Three flights (B458, B459 and B460) had valid trace gas measurements from the whole air sampling system, shown in Fig. 5. Major features, such as increases in VOCs, were consistent during repeat flight circuits. All circuits had peaks in CO (and NO_x if available) mixing ratio(s) and decreases in the ozone mixing ratio when the aircraft was in the London plume, denoted by the letter "X" in Fig. 5a–c. Acetylene (C_2H_2) was elevated in the London plume and was highly correlated with CO ($r^2 = 0.86$) and NO_x ($r^2 = 0.79$). Acetylene is primarily emitted as vehicle exhaust (Fortin et al., 2005) and has a relatively long atmospheric lifetime of approximately 2 months with respect to oxidation by OH (Atkinson, 2000). Figure 5 also shows the ratio of benzene-to-toluene, which is commonly used to determine the air mass photochemical age because of the different atmospheric lifetimes of the two species (e.g., Warneke et al., 2007). The regions with low benzene/toluene ratios and elevated pollutant concentrations coincided

ACPD
11, 30665–30718, 2011

with the location of the aerosol plume predicted by the UK visibility model and expected based on flow patterns from the synoptic re-analysis, i.e., downwind of London. We also observed elevated CO and VOC concentrations away from the London plume together with increased ozone relative to NO_x. These locations had slightly higher benzene/toluene ratios, suggesting they were more aged regional pollution or aged plumes from non-London sources encountered by the aircraft. We identify these features for selected flights in Fig. 5a–c using the letter "Y".

We estimated initial emission ratios for various VOCs relative to acetylene and CO using a simple linear regression approach. Other methods compare VOC ratios to photochemical age (t_{photo}) to account for changes in VOC concentrations with time due to photochemical reactions (e.g., Warneke et al., 2007). We also calculated emission ratios using the photochemical age method, but only report the linear regression results because of uncertainties in the initial benzene-toluene ratio at the source region and the OH radical concentrations. We did use an estimate of photochemical age to examine aerosol properties as a rough function of time. To do so, we assumed a concentration of hydroxyl radical (2×10^6 molecules cm^{-3}) and an assumed initial toluene/benzene ratio of 5 for London needed for the calculation. The absolute accuracy of the photochemical age was not critical to the analysis because we sought to roughly distinguish fresh and aged air masses. Because we ignored the photochemical aging of the initial emissions when determining our emission ratios, they represented a lower bound for species that are rapidly oxidised. We treated VOC sources for the London plume and surrounding regions as the same, even though the sources may be different, but note the regression approach gave greater weight to higher mixing ratio data points in the London plume. We performed the calculations for data combined from all three flights where VOC data from whole air samplers were available (18, 22, and 23 June).

Emission ratios of various VOCs to acetylene determined from linear regression are listed in Table 3 together with an associated measure of correlation (Pearsons r^2). We generally observed lower coefficients of variation for shorter-lived VOCs, such as

ACPD
11, 30665–30718, 2011

isoprene (~2 h; r^2 = 0.35) and *trans*-2-butene (~2 h; r^2 = 0.38) compared to longer-lived VOCs, such as ethane (~3 months; r^2 = 0.86). The coefficients include both plume and non-plume samples collected by the aircraft, so some variability in the relationship between the VOC and acetylene arises from difference in sources as well as age. Correlations were stronger in the plumes, but we do not report any statistical products due to the low ($n < 5$) number of samples within the plumes for each flight.

We compared our results to several previously published emission ratios for cities in the north-eastern US (Warneke et al., 2007), Mexico City (Bon et al., 2011), emissions directly measured from petrol vehicle exhaust (Harley et al., 1992) and ratios we calculated from measurements at two automatic hydrocarbon monitoring sites in London. The London monitoring locations were Marylebone Road in central London, which is classified as a kerb-side site, and Eltham in eastern London, which is classified as a suburban site. We calculated emission ratios by regressing selected VOCs against acetylene for measurements in June and July between 2008 and 2010 to compare to our June 2009 aircraft observations, but unfortunately both sites had measurement gaps during the EM25 campaign.

We compare VOC emission ratios from different studies to each other in Fig. 6. The emission ratios measured by the aircraft were correlated with those determined for the London monitoring sites (Fig. 6g and h), but the ratios measured at the ground sites were approximately twice those measured aloft. Several factors could be responsible for this offset, including different source regions captured by the aircraft measurements versus the ground locations or the limited time coverage of the aircraft measurements compared to the ground measurement locations. Short-chain alkanes (particularly ethane and propane) measured at the Marylebone Road site were the exception to this trend, having much lower ratios compared to those measured by the aircraft and at the suburban site (Fig. 6a and g). The short alkanes have a large evaporative fuel contribution and previous studies have suggested that this explains the lower ratios observed downwind of urban regions compared to vehicle emissions (de Gouw et al., 2005). The aircraft alkane emission ratios were lower than those measured at the suburban

ACPD
11, 30665–30718, 2011

Eltham site (Fig. 6h), which is less vehicle emission dominated than the Marylebone Road location. The alkane emission ratios were also statistically less certain because of the low coefficients of variation observed in both the aircraft and ground monitoring site data.

Warneke et al. (2007) concluded that emissions of aromatics and alkenes are dominated by vehicle exhaust, at least for urban areas in the north-eastern US, based on the relatively good agreement between emission ratios measured in urban outflow and those reported for petrol engine vehicle exhaust by Harley et al. (1992) (Fig. 6f). We found similar agreement between aircraft-measured and vehicle exhaust emission ratios for aromatics, but poorer agreement for alkene emissions (Fig. 6j). We again point to differences in sources and sampling period as potential explanations for the differences we observed. Alkene emission ratios measured at both London ground sites were in excellent agreement with vehicle exhaust (Fig. 6d and e), suggesting that increasing differences in fleet composition in the US and Europe are not affecting emission ratios. For example, diesel consumption in the Greater London region in 2009 was approximately equal to that of petrol (UK Department of Energy and Climate), but it was approximately 15 % of petrol consumption in California in the first quarter of 2011 (California State Board of Equalization).

Despite differences in timing, sampling method and analytical approach, we observed VOC emission ratios in London outflow that are within a factor of two of those reported for the north-eastern US by Warneke et al. (2007) (Fig. 6i). They reported observations within a factor of two of those reported for 39 US cities by Seila et al. (1989). These findings provide further support to recent analyses that indicate VOC emissions from cities, at least in the locations that have been characterised, are generally consistent, despite differences in location, vehicle fleets, and photochemical environments. For example, Parrish et al. (2009) compared relationships between different VOC mixing ratios for observational datasets collected in several mega-cities and in many US cities. They found nearly identical (0.29–0.31) benzene-acetylene ratios in Mexico City, Tokyo, Beijing and 71 US cities (measured in the 1980s), but lower ratios for recent

ACPD
11, 30665–30718, 2011

measurements in the north-eastern US (0.17). Benzene-acetylene ratios we measured in London outflow were even lower than reported for the northeastern US, at 0.11, however the ratios determined for the ground site locations were higher, between 0.3–0.5. Parish et al. (2009) attributed the lower ratios observed in the north-eastern US to targeted benzene reductions following the 1990 Amendments to the Clean Air Act. Similar benzene emission reductions were implemented in the UK in the 1990s and benzene levels in the UK were dropping by approximately 20 % per year until at least 2005 (Dollard et al., 2007). Our own analysis of Marylebone Road data indicated that the ratio of benzene to acetylene since 2000 was approximately constant at ~0.2 until 2008 but has increased to approximately 0.4 since then, which may be related to changes in the vehicle fleet in London. According to Parrish et al. (2009), the similar ratios for various megacity VOC emission ratios across the world result from a combination of the fact that vehicular emissions and associated fuel evaporation dominate emissions and that the hydrocarbon composition of petrol and exhaust emissions is consistent over these urban areas. Though there are some discrepancies in emission ratios measured by the aircraft and those from the ground-based monitoring stations, we found no evidence of a major difference between the London emission ratios and those reported for other highly-developed urban regions.

Isoprene is a major biogenic VOC that also has both vehicular and other anthropogenic sources. Langford et al. (2010) performed eddy covariance VOC flux measurements over London and also analysed long-term Marylebone Road VOC observations to conclude that as much as 80 % of isoprene in London has biogenic sources on warm (30 °C) days. We compared isoprene to benzene (not shown) to identify periods of the flight when isoprene became elevated with respect to benzene. Two portions of different flights showed large increases in isoprene mixing ratios in the absence of changes in benzene and other anthropogenic pollution tracers, both occurring over the southern portion of each flight circuit (Fig. 5). We believe both of these events were associated with increased emissions from the more rural landscape south of the M25 region rather than emissions from London itself based on the wind flow patterns during

ACPD
11, 30665–30718, 2011

each flight. We also observed increases in isoprene mixing ratios over London that were coincident with increases in benzene. Langford et al. (2010) performed a comparison between isoprene and benzene to identify temperature-dependent (i.e., biogenic), non-traffic contributions to isoprene. Average maximum temperatures in London on the days of our measurements were between 18–25 °C, which corresponds to a 20–60 % expected temperature-dependent/biogenic isoprene contribution (Langford et al., 2010). We observed slightly higher isoprene relative to benzene on 23 June (maximum temperature ~25 °C) compared to 22 June (maximum temperature ~22 °C) consistent with this view.

3.3 Aerosol physical properties

Aerosol number distributions measured by the PCASP and CAS wing-mounted probes showed a dominant accumulation mode (centred at approximately 0.17 µm) with only minor contributions from coarse particles (optical diameter >1 µm) to total number and volume during the London circuits. The campaign-averaged standard deviation of the number distributions were best represented by a log-normal distribution with mean diameter 0.17 µm and a standard deviation of 1.4. We observed little change in aerosol number size distributions around the circuit, consistent with relatively homogeneous sub-micron aerosol mass concentrations and light scattering coefficients that were measured by the AMS and nephelometer, respectively. The consistent number distributions also arose partly from their limited size range because they did not measure particles below approximately 0.1 µm diameter and were therefore insensitive to changes in ultrafine particles in the London plume. Changes in total number concentrations measured by the ultrafine CPC (diameter >~3 nm) partly reflected changes in sub-0.1 µm particles because they dominate number distributions, giving us some indication of their distribution around London during the flights. The regions of high particle number concentrations shown in Fig. 7 were not always co-located with the urban plume. We observed a correlation between particle concentrations and sulphur dioxide (SO_2) mixing ratios, particularly downwind of coal-fired power plants in the vicinity of

ACPD
11, 30665–30718, 2011

London, including the Didcot, Tilbury and Kings North power stations shown in Fig. 1b. These observations are consistent with the well-documented formation of fine sulphur containing particles downwind of SO_2 sources (Hewitt, 2001) and indicate that at least under typical summertime conditions power plant can have a similar contribution to particle number as the urban emissions in the London area.

Aerosol dry scattering coefficients were correlated with total sub-micron mass (sum of AMS mass and SP2 rBC) for all five flights (Pearson's $r^2 = 0.70$). The ratio of dry scattering coefficients measured at $\lambda = 550$ nm to sub-micron mass yielded a study-average mass scattering efficiency of $3.4\,m^2\,g^{-1}$, consistent with values expected for sub-micron dominated mixtures of OA, ammonium sulphate and ammonium nitrate. We also calculated the scattering and absorption coefficients from size distributions using Mie theory. The bulk, campaign-average aerosol refractive index and density, estimated from particle composition data by a volume-weighted mixing approach, were $1.59–0.022i$ and $1.63\,g\,cm^{-3}$, respectively. The average mass scattering efficiency determined from the Mie calculations was $3.5\,m^2\,g^{-1}$, in agreement with the measured value. The scattering efficiency around London was lower than the value of $4.5\,m^2\,g^{-1}$ for urban aerosols retrieved over the Paris region by Raut and Chazette (2009).

The humidity-dependence of light scattering coefficients (f(RH)) over London was generally weaker than that measured by the same equipment for a sulphate dominated aerosol over the eastern Pacific, shown in Fig. 8. The f(RH) was similar to that retrieved by Randriamiarisoa et al. (2006) for air masses passing over Paris that originated from the UK, however. The lower humidity-dependence of scattering was consistent with higher mass fractions of relatively hydrophobic OA measured over London compared to the eastern Pacific (Allen et al., 2011). The growth factor differed from ~2/3 of the ammonium sulphate-dominated aerosol sampled over the Pacific, showing the importance of treating the aerosol as an internal rather than external mixture.

Aerosol absorption coefficients were correlated with rBC mass concentrations measured by the SP2 for all five flights (Pearson's $r^2 = 0.67$). The regression for all non-profile measurements yielded an rBC mass absorption efficiency (MAE) at 550 nm

ACPD
11, 30665–30718, 2011

of 10.4 $m^2 g^{-1}$, higher than the 7.5 ± 1.2 $m^2 g^{-1}$ value recommended by Bond and Bergstrom (2006) for uncoated BC particles. Subramanian et al. (2010) reported an MAE of 13.1 $m^2 g^{-1}$ for rBC measured by an SP2 and a 3-wavelength PSAP over and downwind of Mexico City. Their MAE included an SP2 mass scaling factor of 1.3 to account for rBC mass falling outside the detection range of the instrument. When we applied the same correction to our data, we obtained an MAE of 7.8 $m^2 g^{-1}$ for London, almost a factor of two lower than that observed over and downwind of Mexico City. Both field (Lack et al., 2008) and laboratory (Cappa et al., 2008) observations have shown that the PSAP measures erroneously high absorption coefficients for high OA loadings, so the lower MAE observed by the PSAP/SP2 combination over London may be partially due to the lower contribution by OA to sub-micron aerosol mass (~30 %) around London compared to roughly 60 % contribution observed over Mexico City (DeCarlo et al., 2008).

We calculated the aerosol single scattering albedo (ω_0), the ratio of the light scattering coefficient to the light extinction (scattering plus absorption) coefficient, from the corrected PSAP and nephelometer observations at $\lambda = 550$ nm around each circuit. The ω_0 decreased to 0.85 ± 0.03 (mean ±1 standard deviation) in the London plumes from a higher regional background of 0.91 ± 0.05 (Table 4), which was consistent with the higher light-absorbing rBC mass fractions in the plume compared to background regions of the circuit. Raut and Chazette (2007) obtained similar behaviour within and outside of the Paris plume. We investigated the timescales for increases in ω_0 by comparing its measured values to photochemical age for periods with valid whole air canister samples. Single scattering albedo increased from approximately 0.84 at t = 0 to approximately 0.95 at t ~1 day, consistent with the plume versus non-plume differences and the addition of secondary material including SOA indicated by the increase in the OA/CO and sub-micron mass/CO ratios with photochemical age. The regression of ω_0 on photochemical age yielded an increase of approximately 0.001 h^{-1}, but there was considerable variability about the regression (r^2 = 0.25). The total sub-micron mass measured by the AMS normalized by rBC increased from roughly 10 µg µg^{-1} BC

ACPD
11, 30665–30718, 2011

to as much as 50 μg μg^{-1} BC after 40 h, with an average increase of 0.35 h^{-1}.

The addition of secondary material and coagulation processes can lead to changes in the rBC mixing state and coating thickness (Moteki et al., 2007; Schwarz et al., 2008; Subramanian et al., 2010), so we compared one measure of rBC mixing state, the number fraction of "thickly coated" particles to photochemical age. The number fraction of "thickly coated" particles increased from approximately 0.18 at $t = 0$ to a maximum of approximately 0.3 at $t = 45$ h, but there was considerable variability in the data. The average increase was approximately 0.08 % h^{-1}, significantly lower than 2.3 % h^{-1} reported by Moteki et al. (2007). Subramanian et al. (2010) also calculated rates of increase in the thickly coated fraction of 0.2-0.25 % h^{-1} over and downwind of Mexico City, closer to our reported values. One important distinction between our results and those reported by Moteki et al. (2007) and Subramanian et al. (2010) in addition to differences in aerosol and photochemical environment was that we considered the entire rBC population but the previous studies restricted their analyses to rBC particles with a specific mass/size range. There was no evidence of observed changes in rBC mixing state with time causing higher mass absorption efficiencies, which might be expected (Bond et al., 2006). This may have been due to different rBC sources to the plume and non-plume regions sampled, measurement artefacts associated with the PSAP light absorption measurement, or changes in rBC structure. See McMeeking et al. (2011) for a more detailed discussion.

3.4 Aerosol chemical properties

The sub-micron aerosol mass concentrations for the major chemical components are summarized for all flights in Fig. 9 and details for specific circuits are shown in Fig. 10. Total sub-micron mass (calculated from the total mass of aerosol measured by the AMS plus rBC measured by the SP2) was relatively homogeneous around the circuit for all flights. The average difference in mass concentration between the London plume and background regions was 15 %, though the average of the plumes and background

ACPD
11, 30665–30718, 2011

total concentrations were nearly identical. Concentrations were between 4–8 $\mu g\,sm^{-3}$ for the 16 and 18 June flights and were higher, between 8–20 $\mu g\,sm^{-3}$, for the 22–24 June flights. The higher aerosol mass loadings on the 22–24 June flights resulted from transport of pollution from continental Europe, consistent with the elevated CO mixing ratios also observed. The lowest aerosol mass concentrations occurred on 18 June during a period of strong westerly flow following passage of a cold front.

The AMS-measured aerosol composition had roughly similar contributions from nitrate, organic aerosol (OA), ammonium, and sulphate, as shown in Fig. 9, which also gives mass fractions of total sub-micron aerosol for each identified species. We averaged mass concentrations for plume intercepts (determined from elevated CO, NO_x and rBC) and background/upwind locations of each flight. The average contributions from each species to total sub-micron mass in the London plume were approximately 6 % for rBC, 25 % for nitrate, 16 % for ammonium, 24 % for sulphate, and 29 % for OA. The average contributions from each species in the regional background aerosol were 3 % for rBC, 20 % for nitrate, 17 % for ammonium, 31 % for sulphate, and 29 % for OA. Sulphate and OA were the two largest contributors to sub-micron mass for all five flights, but nitrate was elevated in the London plumes compared to the background aerosol. The enhancement of nitrate aerosol in the urban plume was also evident in the positive correlation between nitrate-sulphate ratios and rBC around the circuits (r^2 = 0.42). We normalized by sulphate mass to account for regional contributions to nitrate in the plume, assuming there was no urban sulphate source. The increase in nitrate could have resulted from the new formation of nitric acid via oxidation of nitrogen oxides emitted by the city and combination with urban ammonia emissions or pre-existing agricultural emissions upwind to form ammonium nitrate. In addition, it is possible that re-partitioning of nitrate from super-micron particles that are not detected by the AMS to detectable sub-micron particles was responsible for some of the observed increase. Super-micron/coarse mode nitrate arises from the surface reaction of nitric acid on sea salt aerosol. The lack of a significant super-micron contribution to aerosol volume suggests that re-partitioning is the less likely explanation, but we do

ACPD
11, 30665–30718, 2011

not rule out either possibility.

Dall'Osto et al. (2009) identified two types of nitrate in London using a single particle aerosol mass spectrometer: a "local" nitrate formed in the urban area during the night and a larger-sized "regionally transported" nitrate. Our airborne measurements support both a strong regional contribution to nitrate, evident in the relatively high non-plume legs of the flights, as well as a local contribution. The "local" nitrate source was evident in our daytime measurements because of the lower temperatures and higher relative humidity aloft, discussed in more detail in Section 3.5. Thus, while Dall'Osto et al. (2009) observed a disappearance of the local nitrate during the day that they attributed to increased temperature (resulting in volatilization), decreased relative humidity and changes in the boundary layer depth, we still observed a minor, local source of nitrate from the city. Despite the increase in nitrate, total sub-micron aerosol mass concentrations increased either only slightly or in one case (24 June) decreased in the plume, indicating that sub-micron PM emissions from the city were still minor (15 %) compared to contributions from regional aerosol. Refractory black carbon mass concentrations increased by more than a factor of 2 in the plume, but only represented a small contribution to sub-micron aerosol mass.

Aerosol composition has been previously measured by an AMS over and in the outflow of several major cities (de Gouw and Jimenez, 2009), including Mexico City (DeCarlo et al., 2008). Mexico City is a much larger urban region than London and is confined by topography and influenced by a number of additional sources including wildfires and volcanoes (DeCarlo et al., 2008; Yokelson et al., 2007). Its lower latitude and higher altitude compared to London means more radiation is available for photochemical reactions. DeCarlo et al. (2008) observed average AMS mass concentrations of 26.6 $\mu g\,sm^{-3}$ in the Mexico City basin, of which about 60 % was OA, 23 % nitrate and 7 % by sulphate. The higher average OA mass fraction in Mexico City compared to London (60 % versus 30 %) was not surprising given the large differences in photochemical environments and emissions.

ACPD
11, 30665–30718, 2011

Finer-scale changes in aerosol and trace gas concentrations are shown in Fig. 10, which gives total aerosol concentrations along the flight track for a single circuit around London and time series for periods when the aircraft was flying the circuits. We observed elevated sulphate concentrations in several locations around the circuit for multiple flights, particularly during the southern legs (e.g., points Y on Fig. 10b, c and d). The higher sulphate concentrations observed at point Y on 18 June coincided with elevated sulphur dioxide concentrations (not shown) and the transport predicted from the UK4 model suggested these were emissions from the Southampton area, possibly shipping and/or power-plants. The mean, low-level flow on the 23 and 24 June flights and backward trajectory analysis (not shown) indicated that on these occasions the elevated sulphate concentrations likely resulted from transport from continental Europe, particularly the Netherlands and Belgium regions. Carbon monoxide, NO_x (available 22–24 June only) and rBC were strongly correlated and increased during the London plume intercepts, which are indicated by an "X" in Fig. 10. As noted previously, there was little change in total aerosol mass concentrations, with only minor increases in nitrate and organics during plume intercepts.

Aerosol mass concentrations are often normalized by gas-phase tracers of different emission sources to aid comparisons between measurement locations while accounting for the effects of dilution on absolute concentrations. Increases in the aerosol species relative to a long-lived tracer such as CO reflect secondary production, assuming a constant emission ratio. We examined relationships between aerosol species and trace gas mixing ratios for a subset of three flights that had valid gas-phase chemistry data from whole air canister samples. Nitrate was positively correlated with excess CO, acetylene and other traffic-related VOCs with significantly different relationships inside and outside of the London plume. The average non-plume (photochemical age >50 h) nitrate/CO ratio was 80 $\mu g\,sm^{-3}\,ppmv^{-1}$ (r^2 = 0.69) compared to 20–30 $\mu g\,sm^{-3}\,ppmv^{-1}$ in the plumes, reflecting the enhancement of nitrate relative to CO in aged, regional pollution. OA was also positively correlated with CO (r^2 = 0.50) and had different relationships inside and outside of the London plume.

ACPD
11, 30665–30718, 2011

The average OA/CO ratio for photochemical age > 50 h was ~45 $\mu g\,sm^{-3}\,pmv^{-1}$ but lower (~10 $\mu g\,sm^{-3}\,ppmv^{-1}$) during plume sampling (Table 4). The relationships between nitrate and OA mass concentrations with respect to acetylene, ethane and other long-lived VOCs also showed similar relationships as those observed for CO.

Allan et al. (2010) measured OA and CO in central London and calculated an average OA/CO ratio of 10.30 $\mu g\,sm^{-3}\,ppmv^{-1}$ using linear regression. They restricted their calculation to sub-200 nm diameter OA, but our size-resolved OA data for the circuit flights was too variable to allow a similar calculation. Our observed OA/CO ratio of ~10 $\mu g\,sm^{-3}\,ppmv^{-1}$ in the London plume was similar to the Allan et al. (2010) value despite the larger size range of OA in our calculations. We suspect the addition of OA mass for $D > 200$ nm particles in our calculation was offset by different source footprints. We observed much lower OA/CO ratios in the London plume compared to approximately 80 $\mu g\,sm^{-3}\,ppmv^{-1}$ measured in the Mexico City outflow by DeCarlo et al. (2008). DeCarlo et al. (2008) attributed the high OA/CO ratio to a combination of rapid photochemistry and biomass burning influence. Photochemical reactions likely proceeded more slowly over London compared to Mexico City due to lower trace gas concentrations and reduced actinic flux. de Gouw and Jimenez (2009) summarized recent AMS OA measurements for urban emissions and reported that primary OA/CO ratios were typically between 5–15 $\mu g\,sm^{-3}\,ppmv^{-1}$, in agreement with our London plume measurements. They suspected the lower end of this range was more accurate due to the difficulty in accounting for the rapid formation of SOA and background SOA downwind of urban sources. de Gouw and Jimenez (2009) also examined aged urban air and found that OA/CO was about 70 ± 20 $\mu g\,sm^{-3}\,ppmv^{-1}$ for a wide range of emissions and photochemical environments. Our measured OA/CO ratios in non-plume air around London were also consistent with these results, providing further evidence of the important contributions by SOA, even in regions with large urban emission sources such as north western Europe. We stress that our non-plume and plume sampling did not measure the same air mass or sources, but rather represent the contrast between emissions from a major European megacity (London) with surrounding regional

ACPD
11, 30665–30718, 2011

pollution from a variety of UK and European sources.

Refractory BC is a combustion product produced by vehicle traffic, so we compared its measured mass concentrations to other traffic tracers including CO and certain VOCs. Several previous studies have examined BC/CO relationships and have reported values ranging from ~1–6 ng sm^{-3} ppbv^{-1} (Baumgardner et al., 2007; McMeeking et al., 2010; Spackman et al., 2008; Subramanian et al., 2010). Using whole air canister samples, we observed substantially higher ratios downwind of London, with rBC/CO approximately 10–12 ng sm^{-3} ppbv^{-1}. Refractory BC/CO ratios reflect the mix of sources within the city, and for London we believe the increased contributions from diesel vehicles, which produce relatively more rBC compared to petrol vehicles, explain the higher rBC/CO ratios compared to other locations. Refractory BC was also correlated with other traffic-related and relatively long-lived VOCs, including ethane (r^2 = 0.72) and acetylene (r^2 = 0.81).

3.5 Aerosol vertical structure

Each research flight included vertical profiles from approximately 3000 m to the surface before the first circuit around London in the vicinity of Northolt airfield (Fig. 1). Each profile occurred at approximately 10:00 UTC ±1 h. Potential temperature, potential dew point temperature and aerosol mass concentrations for individual species measured by the AMS and rBC during the profiles are shown in Fig. 11. The planetary boundary layer (PBL) height was about 1900 m for the 16 and 18 June flights. Two distinct layers were visible on the 22 June flight, with a well-mixed layer (constant potential temperature) extending from the surface to approximately 1200 m underneath a warmer (in terms of potential temperature) layer extending up to 2100 m. The upper layer was no longer evident by the 23 June and the mixed layer extended from the surface up to approximately 1400 m. The feature was also apparent during the 24 June flight, with a shallow mixed layer extending from the surface up to 750 m underneath a warmer, deeper layer extending up to 1900 m.

ACPD
11, 30665–30718, 2011

The mass concentrations during the two westerly flights (16 and 18 June) were lower throughout the depth of the PBL compared to the 22–24 June flights. The profiles revealed a more complicated vertical structure for the flights where anti-cyclonic conditions dominated on 22–24 June. Within the PBL, nitrate mass concentrations increased with altitude, as previously observed by Morgan et al. (2009) during similar airborne measurements over the UK. They linked the enhancement of nitrate with altitude to decreases in temperature and increases in RH that altered the equilibrium of the nitric acid-ammonia-ammonium nitrate system towards the particle/ammonium nitrate phase. This is consistent with the increase in nitrate with relative humidity observed during several flights around London. For example, during the 23 June flight (B460), nitrate mass concentrations increased by a factor of 3 for a 40 % increase in RH whereas sulphate and OA concentrations remained constant. Mass concentrations of rBC indicated a more highly polluted layer close to the surface for the 23 and 24 June flights, which corresponded to the shallower, dryer mixed layer. McMeeking et al. (2011) discuss several aspects of the vertical structure of rBC mass concentrations and their physical properties in more detail.

Morgan et al. (2009) also performed a statistical analysis of aerosol composition measured by an AMS from the FAAM research aircraft for more than 300 profiles around the UK coastline. They used a cluster analysis technique to group profiles according to air mass trajectory, which included an Atlantic or westerly cluster, an easterly cluster and a stagnant or low transport cluster. Aerosol concentrations (and nitrate in particular) were generally lower for the Atlantic cluster compared to the easterly and stagnant clusters. Our observations around London show similar results for aerosol concentrations and composition. The two westerly flights (16 and 18 June) feature lower aerosol concentrations compared to the easterly and stagnant cases (22–24 June), with lower nitrate concentrations observed during profiles. Nitrate mass concentrations increased approximately four-fold during profiles in easterly and stagnant conditions compared to westerly, also consistent with the findings of Morgan et al. (2009). Sub-micron mass concentrations during the easterly cases were slightly

ACPD
11, 30665–30718, 2011

higher than the 75th percentile values reported by Morgan et al. (2009), meaning conditions during these flights (22–24 June) represented relatively polluted conditions for the UK, consistent with the ground-based $PM_{2.5}$ statistics (Fig. 3).

The aerosol vertical structure was also probed by the mobile, van-based lidar system, which operated on selected days during the campaign. A separate analysis focuses in detail on the ground-based lidar and on comparisons between the ground-based lidar and aircraft measurements during the campaign and we only include a brief description of some basic results here. Fig. 12 presents an example of a lidar "curtain" measured around the M25 on the same day as flight B457 (16 June). The lidar signals have been calibrated, range-corrected, corrected from the overlap factor and for molecular transmission (Chazette, 2003). The lidar results also showed a relatively homogenous aerosol concentrations along the loop around London, consistent with the aircraft observations of relatively constant mass around the circuit (Fig. 10a).

We compared light scattering coefficients measured during individual aircraft profiles between 0-3 km to lidar-retrieved extinction coefficients averaged over regions in close proximity to the location of the aircraft measurements. Lidar extinction coefficients were retrieved following the procedures described by Raut and Chazette (2007) and Royer et al. (in press), assuming a lidar ratio of 45.5 sr. Fig. 13 shows profile data for two flight days, 16 and 23 June, where the presence of clouds did not complicate the lidar retrievals. We also show altitude-averaged aerosol composition data measured by the AMS and SP2 during each profile. The profiles were flown roughly upwind (northwest for 16 June and east for 23 June) and downwind (northeast for 16 June and northwest for 23 June) of central London. It should be stressed that the aircraft profiles do not represent a perfectly vertical column of the atmosphere, but are spread out in horizontal space as well due to the restrictions on the aircraft flight path. Small scale horizontal features, including plumes, can appear to be a vertical feature for this reason, so some care should be used in interpreting the profile measurements.

The aircraft and lidar measurements showed qualitatively similar results for both flight days and in both the upwind and downwind regions. The 16 June profiles showed a

ACPD
11, 30665–30718, 2011

deeper mixed layer extending to approximately 1.5 km and the 23 June profiles showed a shallower mixed layer extending to approximately 1.2 km. The upwind profiles were lower compared to the downwind profiles in terms of aircraft measured scattering coefficients, aerosol mass and lidar-measured extinction coefficients. The lidar-retrieved extinction coefficients were approximately a factor of two higher than the aircraft measured scattering coefficients. This was more than could be reasonable explained by the contribution of the absorption coefficient, which could not be measured on the aircraft during profiles due to limitations in the PSAP sensitivity and time response. Aerosol single scattering albedo measured in the polluted mixed layer during level flight were between 0.85 to 0.9, so absorption only represented 15 % of the extinction signal at most. The most likely reasons for the higher lidar results stem from the need to bring aerosol into the aircraft for measurement. Ambient particles are exposed to ram heating and heating by the higher cabin temperature, which acts to both dry the particles and potentially remove semi-volatile aerosol components. The sampling efficiency for transmitting the entire aerosol distribution into the aircraft could also affect the agreement. These processes act to lower the scattering coefficient measured on the aircraft compared to that retrieved by the lidar for ambient aerosol. The lidar measurements include contributions by coarse mode particles (though these should be relatively small, 10 %, based on measured size distributions) and more importantly by water and other semi-volatile material associated with the particles. For example, the f(RH) measurements indicate that the scattering coefficient at 80 % RH (typical values during the profiles shown in Fig. 13) was approximately 1.5 times the dry scattering coefficient.

4 Conclusions

We carried out a series of research flights and ground-based lidar van circuits around the mega-city of London. The London plume was clearly visible against a regional background for major vehicle traffic emission tracers, including CO, NO_x, certain VOCs and rBC. There was little change in total aerosol mass concentrations between the ur-

ACPD
11, 30665–30718, 2011

ban plume and the regional, background aerosol, with only minor increases in nitrate observed. Organic aerosol ratios to carbon monoxide in the plume (10 µg sm^{-3} ppbv^{-1}) and in regional aerosol (45 µg sm^{-3} ppbv^{-1}) were similar to other recently reported measurements for urban emissions and regional/aged pollution. There were large increases in rBC mass concentrations but these were a small contributor to total sub-micron mass. Despite its relatively small influence on sub-micron mass, rBC emitted by London resulted in lower aerosol single scattering albedo (plume average of 0.86 versus 0.91 for the regional aerosol), which may have important regional climate effects. VOC emission ratios in London were relatively similar to those measured downwind of major US cities, suggesting similar traffic sources and fuel composition. Comparisons between aircraft-measured vertical profiles and lidar retrieved aerosol showed similar structure. Regional/secondary aerosol dominated urban sources, meaning PM levels in London are largely governed by the influences of meteorology and surrounding emissions rather than directly on sources within London itself.

Acknowledgements. The EM25 campaign was supported by the UK Met Office and the Natural Environment Research Council (NERC) APPRAISE-ADIENT project (NE/E-011101/1). The mobile lidar van was supported by the Commissariat à l'Energie Atomique (CEA). Airborne data were obtained using the BAe-146-301 Atmospheric Research Aircraft (ARA) flown by Directflight Ltd. and managed by the Facility for Airborne Atmospheric Measurements (FAAM), which is a joint entity of the Natural Environment Research Council (NERC) and the Met Office. We thank the FAAM, Directflight and Avalon project partners for their support during the campaign and the FAAM pilots in particular for safely negotiating the busy London airspace. London air quality ground stations are supported by the Environmental Research Group at Kings College London and the Automatic Hydrocarbons Monitoring Network are supported by the Department for Environment, Food and Rural Affairs (DEFRA). We also thank P. I. Williams, G. Capes and M. Flynn for AMS and SP2 instrument support. The NERC National Centre for Atmospheric Sciences supported maintenance of the AMS, the Whole Air Sampling system and the off-line GC analyses. ECMWF reanalysis data were provided by the ERA-Interim data extraction tool.

ACPD
11, 30665–30718, 2011

References

Aiken, A. C., Salcedo, D., Cubison, M. J., Huffman, J. A., DeCarlo, P. F., Ulbrich, I. M., Docherty, K. S., Sueper, D., Kimmel, J. R., Worsnop, D. R., Trimborn, A., Northway, M., Stone, E. A., Schauer, J. J., Volkamer, R. M., Fortner, E., de Foy, B., Wang, J., Laskin, A., Shutthanandan, V., Zheng, J., Zhang, R., Gaffney, J., Marley, N. A., Paredes-Miranda, G., Arnott, W. P., Molina, L. T., Sosa, G., and Jimenez, J. L.: Mexico City aerosol analysis during MILAGRO using high resolution aerosol mass spectrometry at the urban supersite (T0) Part 1: Fine particle composition and organic source apportionment, Atmos. Chem. Phys., 9, 6633–6653, doi:10.5194/acp-9-6633-2009, 2009.

Allan, J. D., Williams, P. I., Morgan, W. T., Martin, C. L., Flynn, M. J., Lee, J., Nemitz, E., Phillips, G. J., Gallagher, M. W., and Coe, H.: Contributions from transport, solid fuel burning and cooking to primary organic aerosols in two UK cities, Atmos. Chem. Phys., 10, 647–668, doi:10.5194/acp-10-647-2010, 2010.

Allen, G., Coe, H., Clarke, A., Bretherton, C., Wood, R., Abel, S. J., Barrett, P., Brown, P., George, R., Freitag, S., McNaughton, C., Howell, S., Shank, L., Kapustin, V., Brekhovskikh, V., Kleinman, L., Lee, Y.-N., Springston, S., Toniazzo, T., Krejci, R., Fochesatto, J., Shaw, G., Krecl, P., Brooks, B., McMeeking, G., Bower, K. N., Williams, P. I., Crosier, J., Crawford, I., Connolly, P., Allan, J. D., Covert, D., Bandy, A. R., Russell, L. M., Trembath, J., Bart, M., McQuaid, J. B., Wang, J., and Chand, D.: South East Pacific atmospheric composition and variability sampled along 20 S during VOCALS-REx, Atmos. Chem. Phys., 11, 5237–5262, doi:10.5194/acp-11-5237-2011, 2011.

Anderson, T. L. and Ogren, J. A.: Determining Aerosol Radiative Properties Using the TSI 3563 Integrating Nephelometer, Aerosol. Sci. Tech., 29, 57–69, doi:10.1080/02786829808965551, 1998.

Atkinson, R.: Atmospheric chemistry of VOCs and NO_x, Atmos. Environ., 34, 2063–2101, doi:10.1016/S1352-2310(99)00460-4, 2000.

Atkinson, R. W., Barratt, B., Armstrong, B., Anderson, H. R., Beevers, S. D., Mudway, I. S., Green, D., Derwent, R. G., Wilkinson, P. and Tonne, C.: The impact of the congestion charging scheme on ambient air pollution concentrations in London, Atmos. Environ., 43, 5493–5500, doi:10.1016/j.atmosenv.2009.07.023, 2009.

Banta, R. M., Senff, C. J., Nielsen-Gammon, J., Darby, L. S., Ryerson, T. B., Alvarez, R. J., Sandberg, S. P., Williams, E. J. and Trainer, M.: A Bad Air Day in Houston, B. Am. Meteorol.

ACPD
11, 30665–30718, 2011

Soc., 86, 657, doi:10.1175/BAMS-86-5-657, 2005.
Baumgärdner, D., Kok, G., and Raga, G.: Warming of the Arctic lower stratosphere by light absorbing particles, Geophys. Res. Lett., 31, L06117, doi:10.1029/2003GL018883, 2004.
Baumgärdner, D., Kok, G. L., and Raga, G. B.: On the diurnal variability of particle properties related to light absorbing carbon in Mexico City, Atmos. Chem. Phys., 7, 2517–2526, doi:10.5194/acp-7-2517-2007, 2007.
Bigi, A. and Harrison, R. M.: Analysis of the air pollution climate at a central urban background site, Atmos. Environ., 44, 2004–2012, doi:10.1016/j.atmosenv.2010.02.028, 2010.
Bon, D. M., Ulbrich, I. M., de Gouw, J. A., Warneke, C., Kuster, W. C., Alexander, M. L., Baker, A., Beyersdorf, A. J., Blake, D., Fall, R., Jimenez, J. L., Herndon, S. C., Huey, L. G., Knighton, W. B., Ortega, J., Springston, S., and Vargas, O.: Measurements of volatile organic compounds at a suburban ground site (T1) in Mexico City during the MILAGRO 2006 campaign: measurement comparison, emission ratios, and source attribution, Atmos. Chem. Phys., 11, 2399–2421, doi:10.5194/acp-11-2399-2011, 2011.
Bond, C. M., Anderson, T. L., Campbell, D., and Bond, T. C.: Calibration and intercomparison of filter-based measurements of visible light absorption by aerosols, Aerosol Sci. Tech., 30, 582–600, 1999.
Bond, T. C., Habib, G., and Bergstrom, R. W.: Limitations in the enhancement of visible light absorption due to mixing state, J. Geophys. Res., 111, D20211, doi:10.1029/2006JD007315, 2006.
Bond, T. and Bergström, R.: Light Absorption by Carbonaceous Particles: An Investigative Review, Aerosol Sci. Technol., 40, 27–67, doi:10.1080/02786820500421521, 2006.
Canagaratna, M. R., Jayne, J. T., Jimenez, J. L., Allan, J. D., Alfarra, M. R., Zhang, Q., Onasch, T. B., Drewnick, F., Coe, H., Middlebrook, A., Delia, A., Williams, L. R., Trimborn, A. M., Northway, M. J., DeCarlo, P. F., Kolb, C. E., Davidovits, P., and Worsnop, D. R.: Chemical and microphysical characterization of ambient aerosols with the aerodyne aerosol mass spectrometer, Mass. Spectrom. Rev., 26, 185–222, 2007.
Cappa, C. D., Lack, D. A., Burkholder, J. B. and Ravishankara, A. R.: Bias in filter-based aerosol light absorption measurements due to organic aerosol loading: Evidence from laboratory measurements, Aerosol Sci. Technol., 42, 1022–1032, doi:10.1080/02786820802389285, 2008.
Chazette, P.: The monsoon aerosol extinction properties at Goa during INDOEX as measured with lidar, J. Geophys. Res., 108, 4187, doi:10.1029/2002JD002074, 2003.

ACPD
11, 30665–30718, 2011

Chazette, P., Randriamiarisoa, H., Sanak, J. and Couvert, P.: Optical properties of urban aerosol from airborne and ground-based in situ measurements performed during the Etude et Simulation de la Qualité de l'air en Ile de France (ESQUIF) program, J. Geophys. Res., 110, D02206, doi:10.1029/2004JD004810, 2005.

Chazette, P., Sanak, J. and Dulac, F.: New approach for aerosol profiling with a Lidar onboard an ultralight aircraft: Application to the African Monsoon Multidisciplinary Analysis, Environ. Sci. Technol., 41, 8335–8341, 2007.

Clark, P. A., Harcourt, S. A., Macpherson, B., Mathison, C. T., Cusack, S. and Naylor, M.: Prediction of visibility and aerosol within the operational Met Office Unified Model. I?: Model formulation and variational assimilation, Q. J. Roy. Meteor. Soc., 134, 1801–1816, doi:10.1002/qj.318, 2008.

Dall'Osto, M., Harrison, R. M., Coe, H., Williams, P. I., and Allan, J. D.: Real time chemical characterization of local and regional nitrate aerosols, Atmos. Chem. Phys., 9, 3709–3720, doi:10.5194/acp-9-3709-2009, 2009.

Davies, L., Bell, J. N. B., Bone, J., Head, M., Hill, L., Howard, C., Hobbs, S. J., Jones, D. T., Power, S. a, Rose, N., Ryder, C., Seed, L., Stevens, G., Toumi, R., Voulvoulis, N., and White, P. C. L.: Open Air Laboratories (OPAL): A community-driven research programme, Environ. Poll., 159, 2203–2210, doi:10.1016/j.envpol.2011.02.053, 2011.

DeCarlo, P. F., Dunlea, E. J., Kimmel, J. R., Aiken, A. C., Sueper, D., Crounse, J., Wennberg, P. O., Emmons, L., Shinozuka, Y., Clarke, A., Zhou, J., Tomlinson, J., Collins, D. R., Knapp, D., Weinheimer, A. J., Montzka, D. D., Campos, T., and Jimenez, J. L.: Fast airborne aerosol size and chemistry measurements above Mexico City and Central Mexico during the MILAGRO campaign, Atmos. Chem. Phys., 8, 4027–4048, doi:10.5194/acp-8-4027-2008, 2008.

Dollard, G. J., Dumitrean, P., Telling, S., Dixon, J., and Derwent, R. G.: Observed trends in ambient concentrations of C2–C8 hydrocarbons in the United Kingdom over the period from 1993 to 2004, Atmos. Environ., 41, 2559–2569, doi:10.1016/j.atmosenv.2006.11.020, 2007.

Draxler, R. R. and Rolph, G. D.: HYSPLIT (Hybrid Single-Particle Lagrangian Integrated Trajectory) Model access via NOAA ARL READY website (http://ready.arl.noaa.gov/HYSPLIT.php), 2011.

Drewnick, F., Hings, S. S., Decarlo, P., Jayne, J. T., Gonin, M., Fuhrer, K., Weimer, S., Jimenez, J. L., Borrmann, K. L. D. S. and Worsnop, D. R.: A new time-of-flight aerosol mass spectrometer (TOF-AMS)-Instrument description and first field deployment, Aerosol Sci. Technol., 39, 637–658, doi:101080/02786820500182040, 2005.

ACPD
11, 30665–30718, 2011

Fortin, T. J., Howard, B. J., Parrish, D. D., Goldan, P. D., Kuster, W. C., Atlas, E. L. and Harley, R. A.: Temporal changes in U.S. benzene emissions inferred from atmospheric measurements., Environ. Sci. Technol., 39, 1403–1408, 2005.

Fuller, G. W. and Green, D.: Evidence for increasing concentrations of primary PM10 in London, Atmos. Environ., 40, 6134–6145, doi:10.1016/j.atmosenv.2006.05.031, 2006.

Garland, R. M., Yang, H., Schmid, O., Rose, D., Nowak, A., Achtert, P., Wiedensohler, A., Takegawa, N., Kita, K., Miyazaki, Y., Kondo, Y., Hu, M., Shao, M., Zeng, L. M., Zhang, Y. H., Andreae, M. O., and Pöschl, U.: Aerosol optical properties in a rural environment near the mega-city Guangzhou, China: implications for regional air pollution, radiative forcing and remote sensing, Atmos. Chem. Phys., 8, 5161–5186, doi:10.5194/acp-8-5161-2008, 2008.

de Gouw, J. and Jimenez, J. L.: Organic aerosols in the Earth's atmosphere, Environ. Sci. Technol., 43, 7614–7618, doi:10.1021/es9006004, 2009.

de Gouw, J. A., Middlebrook, A. M., Warneke, C., Goldan, P. D., Kuster, W. C., Roberts, J. M., Fehsenfeld, F. C., Worsnop, D. R., Canagaratna, M. R., Pszenny, A. A. P., Keene, W. C., Marchewka, M., Bertman, S. B., and Bates, T. S.: Budget of organic carbon in a polluted atmosphere: Results from the New England Air Quality Study in 2002, J. Geophys. Res., 110, D16305, doi:10.1029/2004JD005623, 2005.

Harley, R. A., Hannigan, M. P. and Cass, G. R.: Respeciation of organic gas emissions and the detection of excess unburned gasoline in the atmosphere, Environ. Sci. Technol., 26, 2395–2408, doi:10.1021/es00036a010, 1992.

Harrison, R. M., Jones, A. M., and Lawrence, R. G.: Major component composition of PM10 and $PM_{2.5}$ from roadside and urban background sites, Atmos. Environ., 38, 4531–4538, doi:10.1016/j.atmosenv.2004.05.022, 2004.

Haywood, J., Francis, P., Osborne, S., Glew, M., Loeb, N., Highwood, E., Tanre, D., Myhre, G., Formenti, P. and Hirst, E.: Radiative properties and direct radiative effect of Saharan dust measured by the C-130 aircraft during SHADE: 1. Solar spectrum, J. Geophys. Res., 108, 1423–1447, doi:10.1029/2002JD002687, 2003.

Haywood, J. M., Pelon, J., Formenti, P., Bharmal, N., Brooks, M., Capes, G., Chazette, P., Chou, C., Christopher, S., Coe, H., Cuesta, J., Derimian, Y., Desboeufs, K., Greed, G., Harrison, M., Heese, B., Highwood, E. J., Johnson, B., Mallet, M, Marticorena, B., Marsham, J., Milton, S., Myhre, G., Osborne, S. R., Parker, D. J., Rajot, J.-L., Schulz, M., Slingo, A., Tanre, D., and Tulet, P.: Overview of the Dust and Biomass-burning Experiment and African Monsoon Multidisciplinary Analysis Special Observing Period-0, J. Geophys. Res.,

ACPD
11, 30665–30718, 2011

113, D00C17, doi:10.1029/2008JD010077, 2008a.
Haywood, J., Bush, M., Abel, S., Claxton, B., Coe, H., Crosier, J., Harrison, M., Macpherson, B., Naylor, M. and Osborne, S.: Prediction of visibility and aerosol within the operational Met Office Unified Model II?: Validation of model performance using observational data, Q. J. Roy. Meteor. Soc., 134, 1817–1832, doi:10.1002/qj.275, 2008b.
Hewitt, C. N.: The atmospheric chemistry of sulphur and nitrogen in power station plumes, Atmos. Environ., 35, 1155–1170, doi:10.1016/S1352-2310(00)00463-5, 2001.
Hopkins, J. R., Boddy, R. K., Hamilton, J. F., Lee, J. D., Lewis, A. C., Purvis, R. M., and Watson, N. J.: An observational case study of ozone and precursors inflow to South East England during an anticyclone, J. Environ. Monitor., 8, 1195–202, doi:10.1039/b608062f, 2006.
Hopkins, J. R., Jones, C. E., and Lewis, A. C.: A dual channel gas chromatograph for atmospheric analysis of volatile organic compounds including oxygenated and monoterpene compounds., J. Environ. Monitor., 13, 2268–2276, doi:10.1039/c1em10050e, 2011.
Lack, D. A., Cappa, C. D., Covert, D. S., Baynard, T., Massoli, P., Sierau, B., Bates, T. S., Quinn, P. K., Lovejoy, E. R., Ravishankara, A. R. and Burkholder, J. B.: Bias in filter-based aerosol light absorption measurements due to organic aerosol loading: Evidence from laboratory measurements, Aerosol Sci. Technol., 42, 1033–1041, 2008.
Langford, B., Nemitz, E., House, E., Phillips, G. J., Famulari, D., Davison, B., Hopkins, J. R., Lewis, A. C., and Hewitt, C. N.: Fluxes and concentrations of volatile organic compounds above central London, UK, Atmos. Chem. Phys., 10, 627–645, doi:10.5194/acp-10-627-2010, 2010.
Lawrence, M. G., Butler, T. M., Steinkamp, J., Gurjar, B. R., and Lelieveld, J.: Regional pollution potentials of megacities and other major population centers, Atmos. Chem. Phys., 7, 3969–3987, doi:10.5194/acp-7-3969-2007, 2007.
McMeeking, G. R., Hamburger, T., Liu, D., Flynn, M., Morgan, W. T., Northway, M., Highwood, E. J., Krejci, R., Allan, J. D., Minikin, A., and Coe, H.: Black carbon measurements in the boundary layer over western and northern Europe, Atmos. Chem. Phys., 10, 9393–9414, doi:10.5194/acp-10-9393-2010, 2010.
McMeeking, G. R., Morgan, W. T., Flynn, M., Highwood, E. J., Turnbull, K., Haywood, J., and Coe, H.: Black carbon aerosol mixing state, organic aerosols and aerosol optical properties over the United Kingdom, Atmos. Chem. Phys., 11, 9037–9052, doi:10.5194/acp-11-9037-2011, 2011.
Menut, L., Vautard, R., Flamant, C., Abonnel, C., Beekmann, M., Chazette, P., Flamant, P. H.,

ACPD
11, 30665–30718, 2011

Gombert, D., Gudalia, D., Kley, D., Lefebvre, M. P., Lossec, B., Martin, D., Mgie, G., Perros, P., Sicard, M., and Toupance, G.: Measurements and modelling of atmospheric pollution over the Paris area: an overview of the ESQUIF Project, Ann. Geophys., 18, 1467–1481, doi:10.1007/s00585-000-1467-y, 2000.

Molina, M. J. and Molina, L. T.: Megacities and atmospheric pollution, J. Air Waste Manage., 54, 644–680, 2004.

Molina, L. T., Madronich, S., Gaffney, J. S., Apel, E., de Foy, B., Fast, J., Ferrare, R., Herndon, S., Jimenez, J. L., Lamb, B., Osornio-Vargas, A. R., Russell, P., Schauer, J. J., Stevens, P. S., Volkamer, R., and Zavala, M.: An overview of the MILAGRO 2006 Campaign: Mexico City emissions and their transport and transformation, Atmos. Chem. Phys., 10, 8697-8760, doi:10.5194/acp-10-8697-2010, 2010.

Morgan, W. T., Allan, J. D., Bower, K. N., Capes, G., Crosier, J., Williams, P. I., and Coe, H.: Vertical distribution of sub-micron aerosol chemical composition from North-Western Europe and the North-East Atlantic, Atmos. Chem. Phys., 9, 5389–5401, doi:10.5194/acp-9-5389-2009, 2009.

Morgan, W. T., Allan, J. D., Bower, K. N., Esselborn, M., Harris, B., Henzing, J. S., Highwood, E. J., Kiendler-Scharr, A., McMeeking, G. R., Mensah, A. A., Northway, M. J., Osborne, S., Williams, P. I., Krejci, R., and Coe, H.: Enhancement of the aerosol direct radiative effect by semi-volatile aerosol components: airborne measurements in North-Western Europe, Atmos. Chem. Phys., 10, 8151–8171, doi:10.5194/acp-10-8151-2010, 2010a.

Morgan, W. T., Allan, J. D., Bower, K. N., Highwood, E. J., Liu, D., McMeeking, G. R., Northway, M. J., Williams, P. I., Krejci, R., and Coe, H.: Airborne measurements of the spatial distribution of aerosol chemical composition across Europe and evolution of the organic fraction, Atmos. Chem. Phys., 10, 4065–4083, doi:10.5194/acp-10-4065-2010, 2010b.

Moteki, N. and Kondo, Y.: Effects of Mixing State on Black Carbon Measurements by Laser-Induced Incandescence, Aerosol Sci. Technol., 41, 398–417, doi:10.1080/02786820701199728, 2007.

Moteki, N., Kondo, Y., Miyazaki, Y., Takegawa, N., Komazaki, Y., Kurata, G., Shirai, T., Blake, D. R., Miyakawa, T. and Koike, M.: Evolution of mixing state of black carbon particles: Aircraft measurements over the western Pacific in March 2004, Geophys. Res. Lett., 34, L11803, doi:10.1029/2006GL028943, 2007.

Parekh, P.: Ambient air quality of two metropolitan cities of Pakistan and its health implications, Atmos. Environ., 35, 5971–5978, doi:10.1016/S1352-2310(00)00569-0, 2001.

ACPD

11, 30665–30718, 2011

Parrish, D. D., Kuster, W. C., Shao, M., Yokouchi, Y., Kondo, Y., Goldan, P. D., de Gouw, J. a, Koike, M. and Shirai, T.: Comparison of air pollutant emissions among mega-cities, Atmos. Environ., 43, 6435–6441, doi:10.1016/j.atmosenv.2009.06.024, 2009.

Randriamiarisoa, H., Chazette, P., Couvert, P., Sanak, J., and Mégie, G.: Relative humidity impact on aerosol parameters in a Paris suburban area, Atmos. Chem. Phys., 6, 1389–1407, doi:10.5194/acp-6-1389-2006, 2006.

Raut, J.-C. and Chazette, P.: Retrieval of aerosol complex refractive index from a synergy between lidar, sunphotometer and in situ measurements during LISAIR experiment, Atmos. Chem. Phys., 7, 2797–2815, doi:10.5194/acp-7-2797-2007, 2007.

Raut, J.-C. and Chazette, P.: Assessment of vertically-resolved PM10 from mobile lidar observations, Atmos. Chem. Phys., 9, 8617–8638, doi:10.5194/acp-9-8617-2009, 2009.

Royer, P., Chazette, P., Lardier, M. and Sauvage, L.: Aerosol content survey by mini N2-Raman lidar: Application to local and long-range transport aerosols, Atmos. Environ., 45, doi:10.1016/j.atmosenv.2010.11.001, 7487–7495, 2011.

Royer, P., Chazette, P., S artelet, K., Zhang, Q. J., Beekmann, M., and Raut, J.-C.: Lidar-derived PM_{10} and comparison with regional modeling in the frame of the MEGAPOLI Paris summer campaign, Atmos. Chem. Phys. Discuss., 11, 11861–11909, doi:10.5194/acpd-11-11861-2011, 2011.

Ryder, C. L. and Toumi, R.: An urban solar flux island: Measurements from London, Atmos. Environ., 45, 3414–3423, doi:10.1016/j.atmosenv.2011.03.045, 2011.

Schwarz, J. P., Gao, R. S., Fahey, D. W., Thomson, D. S., Watts, L. A., Wilson, J. C., Reeves, J. M., Darbeheshti, M., Baumgardner, D. G., Kok, G. L., Chung, S. H., Schulz, M., Hendricks, J., Lauer, A., Karcher, B., Slowik, J. G., Rosenlof, K. H., Thompson, T. L., Langford, A. O., Loewenstein, M. and Aikin, K. C.: Single-particle measurements of midlatitude black carbon and light-scattering aerosols from the boundary layer to the lower stratosphere, J. Geophys. Res., 111, D16207, doi:10.1029/2006JD007076, 2006.

Schwarz, J. P., Spackman, J. R., Fahey, D. W., Gao, R. S., Lohmann, U., Stier, P., Watts, L. A., Thomson, D. S., Lack, D. A., Pfister, L., Mahoney, M. J., Baumgardner, D., Wilson, J. C. and Reeves, J. M.: Coatings and their enhancement of black carbon light absorption in the tropical atmosphere, J. Geophys. Res., 113, D03203, doi:10.1029/2007JD009042, 2008.

Seila, R. L., Lonneman, W. A., and Meeks, S. A.: Determination of C2 to C12 ambient air hydrocarbons in 39 U.S. cities, from 1984 through 1986, US Environmental Protection Agency, Washington, DC, USA, 1989.

ACPD
11, 30665–30718, 2011

Spackman, J. R., Schwarz, J. P., Gao, R. S., Watts, L. A., Thomson, D. S., Fahey, D. W., Holloway, J. S., de Gouw, J. A., Trainer, M. and Ryerson, T. B.: Empirical correlations between black carbon aerosol and carbon monoxide in the lower and middle troposphere, Geophys. Res. Lett., 35, L19816, doi:10.1029/2008GL035237, 2008.

Subramanian, R., Kok, G. L., Baumgardner, D., Clarke, A., Shinozuka, Y., Campos, T. L., Heizer, C. G., Stephens, B. B., de Foy, B., Voss, P. B., and Zaveri, R. A.: Black carbon over Mexico: the effect of atmospheric transport on mixing state, mass absorption cross-section, and BC/CO ratios, Atmos. Chem. Phys., 10, 219–237, doi:10.5194/acp-10-219-2010, 2010.

Visschedijk, A., Zandveld, P. and Van Der Gon, H. D.: A high resolution gridded European emission database for the EU integrated project GEMS, Apeldoorn, The Netherlands, 2007.

Warneke, C., McKeen, S. A., de Gouw, J. A., Goldan, P. D., Kuster, W. C., Holloway, J. S., Williams, E. J., Lerner, B. M., Parrish, D. D., Trainer, M., Fehsenfeld, F. C., Kato, S., Atlas, E. L., Baker, A., and Blake, D. R.: Determination of urban volatile organic compound emission ratios and comparison with an emissions database, J. Geophys. Res., 112, D10S47, doi:10.1029/2006JD007930, 2007.

Yokelson, R. J., Urbanski, S. P., Atlas, E. L., Toohey, D. W., Alvarado, E. C., Crounse, J. D., Wennberg, P. O., Fisher, M. E., Wold, C. E., Campos, T. L., Adachi, K., Buseck, P. R., and Hao, W. M.: Emissions from forest fires near Mexico City, Atmos. Chem. Phys., 7, 5569–5584, doi:10.5194/acp-7-5569-2007, 2007.

ACPD
11, 30665–30718, 2011

Table 1. Summary of flights and synoptic conditions during the EM25 campaign.

Flight ID	Date	Time (UTC)	Regions sampled	Synoptic flow (850 hPa)
B457	16 June 2009	09:10–14:00	M25 circuits only	light westerly
B458	18 June 2009	09:50–14:45	M25 circuit and SE English coast	strong westerly
B459	22 June 2009	09:10–13:00	M25 circuits only	stagnant/light northerly
B460	23 June 2009	10:00–14:10	M25 circuits only	light easterly
B461	24 June 2009	08:45–12:00	M25 and English channel	strong easterly

ACPD
11, 30665–30718, 2011

Table 2. Summary of in situ trace gas and aerosol sampling instrumentation on the FAAM BAe-146 during the EM25 campaign.

Quantity measured	Instrument	Size range or wavelength
CO	Aero-laser 5002	N/A
NO, NO_2	Thermo model 42	N/A
O_3	Thermo model 49C	N/A
C_2–C_8 volatile organic compounds	whole air sampler (WAS) + off-line gas chromatography	N/A
aerosol composition and mass	Aerodyne time-of-flight aerosol mass spectrometer (AMS)	~ 50 – 800 nm
refractory black carbon aerosol mass	DMT single particle soot photometer (SP2)	~ 70 – 600 nm
aerosol optical diameter and concentration	passive cavity aerosol spectrometer probe (PCASP-100X, SPP200); cloud aerosol spectrometer (CAS)	0.1–3 µm; 0.5–50 µm
aerosol concentration	TSI 3786 water-based ultrafine condensation particle counter (WCPC)	> 3 nm
dry aerosol light scattering coefficient	TSI 3563 integrating nephelometer	λ = 450, 550, 700 nm
"wet" aerosol light scattering coefficient	"wet" TSI 3563 integrating nephelometer	λ = 450, 550, 700 nm
aerosol light absorption coefficient	particle soot absorption photometer (PSAP)	λ = 567 nm (corrected to 550 nm)

ACPD
11, 30665–30718, 2011

Table 3. Emission ratios for selected volatile organic compounds with respect to acetylene measured during EM25 and associated coefficient of variation. Atmospheric lifetimes with respect to oxidation by OH at a concentration of 2×10^6 molecules cm^{-3} reported by Atkinson (2000) are listed for selected species.

VOC	τ^1	X/C_2H_2	r^2
acetylene	2 mo	1.0	1.0
ethane	3 mo	3.09	*0.86*
n-butane	4.7 d	1.27	*0.75*
propane	10 d	1.24	*0.43*
iso-butane	7.5 d	0.74	*0.86*
iso-pentane	5 d	0.73	*0.57*
toluene	1.9 d	0.55	*0.90*
ethene	1.4 d	0.52	*0.77*
m + *p*-xylene	5.9 h	0.27	*0.84*
n-pentane	5 d	0.23	*0.32*
2, 3-methylpentane		0.19	*0.67*
benzene	9.4 d	0.11	*0.91*
propene	5.3 h	0.10	*0.60*
ethylbenzene		0.07	*0.51*
n-hexane		0.07	*0.61*
isoprene	1.4 h	0.06	*0.35*
cyclopentane		0.05	*0.55*
o-xylene		0.03	*0.01*
1-butene		0.02	*0.50*
trans-2-butene	2.2 h	0.01	*0.38*
cis-2-butene		0.00	*0.46*

ACPD
11, 30665–30718, 2011

Table 4. Average OA/CO, rBC/CO, single scattering albedo (ω_0) and mass absorption efficiency (MAE) for plume and non-plume periods determined from the photochemical age calculated from whole air canister toluene and benzene mixing ratios. Only flights with valid canister data are listed.

Date	Flight ID	OA/ΔCO [μg sm^{-3} ppbv^{-1}]	rBC/ΔCO [ng sm^{-3} ppbv^{-1}]	ω_0	MAE [m^2 g^{-1}]	# samples
Plumes (t_{photo} <20 h)						
18 June	B458	13	13.1	0.86	6.0	2
21 June	B459	6.8 ± 6.5	8.6 ± 2.0	0.88 ± 0.03	11.6 ± 1.5	6
22 June	B460	8.1 ± 3.2	12.0 ± 1.8	0.84 ± 0.03	9.1 ± 0.8	12
	Average	9.3 ± 3.3	11.2 ± 2.3	0.86 ± 0.02	8.9 ± 2.8	20
Non-plume/background (t_{photo} >50 h)						
18 June	B458	54 ± 11	11.0 ± 1.5	0.93 ± 0.03	9.2 ± 1.9	17
21 June	B459	30 ± 19	10.3 ± 1.9	0.94 ± 0.007	3.7 ± 2	5
22 June	B460	64 ± 9	9.3 ± 0.8	0.86 ± 0.04	5.9 ± 8.4	8
	Average	49 ± 17	10.2 ± 0.9	0.91 ± 0.04	6.3 ± 2.8	30

ACPD
11, 30665–30718, 2011

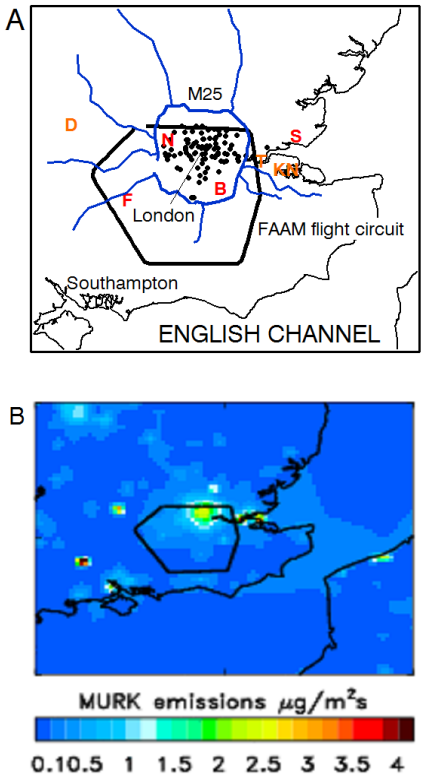

Fig. 1. Maps of south-eastern England showing: **(a)** location of the major motorway network (blue lines), London Air Quality Network observing sites (black circles), the main FAAM London circuit flight track (black line), the locations of three large coal-fired power stations (orange letters: "D" = Didcot; "T" = Tillbury; "KN" = Kings North) and airfields used for missed approaches (red letters: "N" = Northolt; "F" = Farnborough; "B" = Biggin Hill; "S" = Southend) and **(b)** "MURK" emissions (a generic term for emissions that drive the aerosol field in the UK4 model forecast).

ACPD
11, 30665–30718, 2011

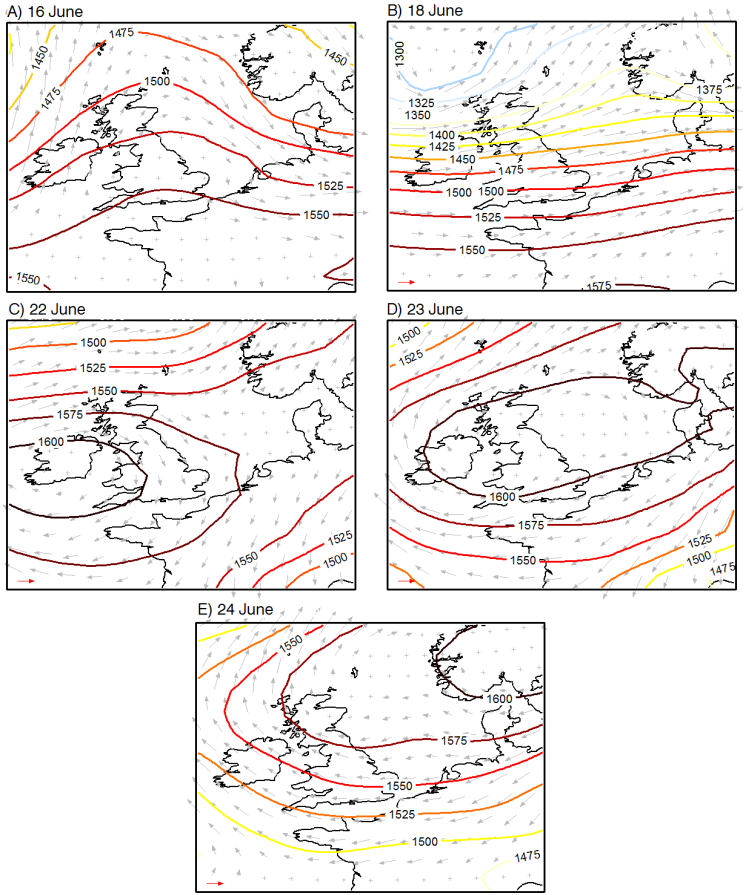

Fig. 2. Maps showing geopotential height and winds from the ERA Interim ECMWF re-analysis at the 850 hPa pressure level at 12:00 UTC for each flight day. Red arrow in lower left-hand corner indicates 10 m s^{-1} wind speed.

ACPD
11, 30665–30718, 2011

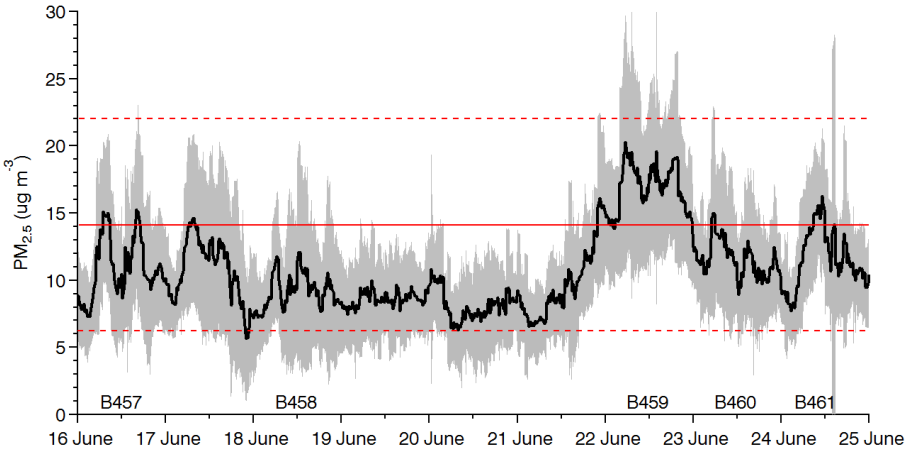

Fig. 3. Time series showing $PM_{2.5}$ concentrations for the EM25 campaign period in 2009. Heavy black line shows London average for all PM stations over the EM25 campaign and grey shading shows one standard deviations of the average. Solid red line shows the June/July historical London average $PM_{2.5}$ concentration from 2005 to 2009 (all station classifications) and dashed red lines show two standard deviations. Flight identification numbers indicates days when the FAAM BAe-146 research aircraft flew circuits over London. Date ticks are labelled at 00:00 for that day.

ACPD
11, 30665–30718, 2011

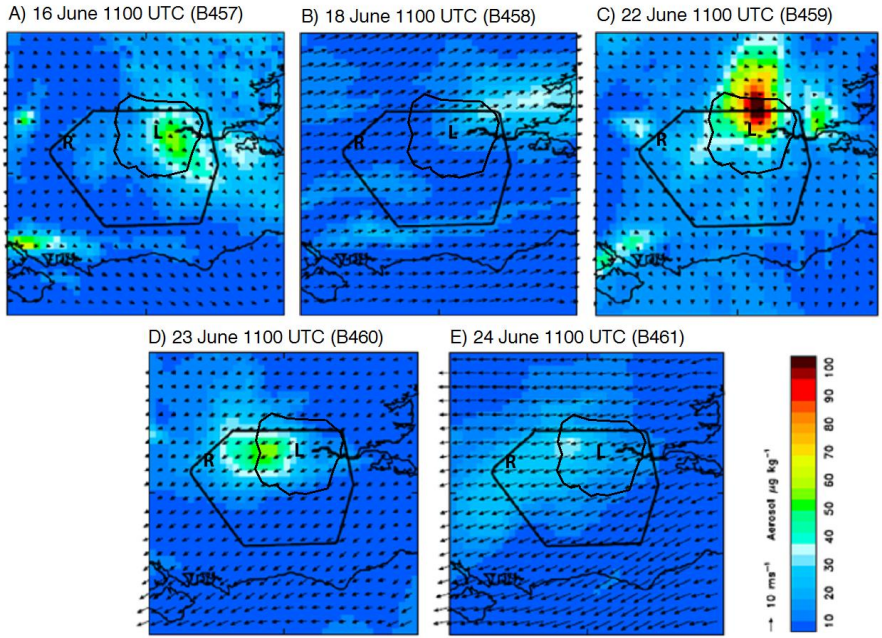

Fig. 4. Aerosol mass mixing ratios predicted at the 760 m altitude by the UK 4km visibility model for selected times during each flight day. Arrows indicate wind speed and direction at the predicted level. The "R" indicates the location of the city of Reading and "L" indicates the location of central London.

ACPD
11, 30665–30718, 2011

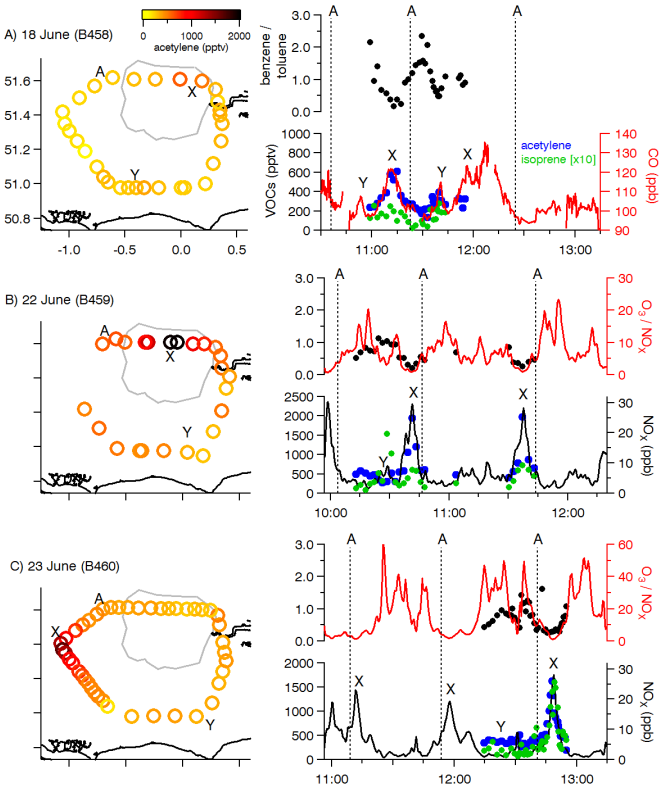

Fig. 5. Mixing ratios for acetylene (C_2H_2), isoprene, nitrogen oxides (NO_x), carbon monoxide and ratios of ozone-to-nitrogen and benzene-to-toluene measured around London for three EM25 flights. NO_x mixing ratios were unavailable for the 18 June flight so CO is shown instead. The approximate location of the London plume is indicated by 'X'. Additional features of interest are shown by "Y". Point 'A' on each map corresponds to the dashed lines on each time series. The flight direction for all days was anti-clockwise.

ACPD
11, 30665–30718, 2011

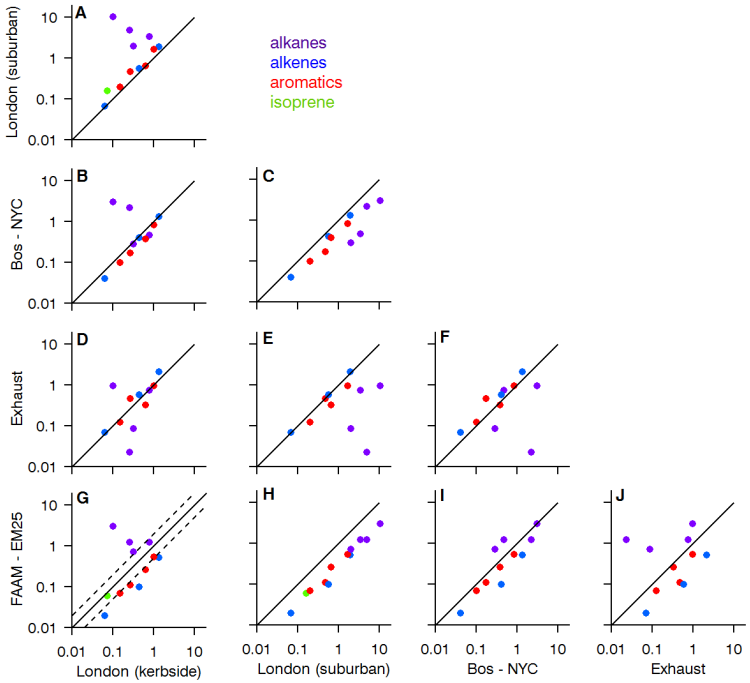

Fig. 6. Selected volatile organic compound (VOC) emission ratios to acetylene (C_2H_2) measured on the FAAM BAe-146 research aircraft, at ground sampling sites in London, and by previous measurement campaigns. Bos-NYC refers to emission ratios measured in the outflow of the north-eastern US reported by Warneke et al. (2007), exhaust refers to vehicle exhaust emission ratios reported by Harley et al. (1992), and the London (kerbside) and London (suburban) data were obtained from the Marylebone Road and Eltham automated hydrocarbon monitoring network locations for June/July 2008-2010. Points are shaded by VOC family as alkanes, alkenes and aromatics. The solid line in panel **(g)** gives the 1:1 relationship and the dashed lines 2:1 and 1:2 relationships; all axes are log-scaled and identical.

ACPD
11, 30665–30718, 2011

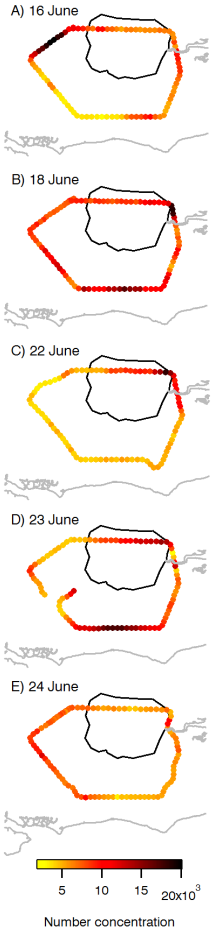

Fig. 7. Number concentrations for particles with $D_p > 3$ nm measured by the ultrafine water-based condensation particle counter for single circuits around London during each flight. Note scale on panel **(d)** has been adjusted by a factor of 2 (maximum N = 40 000 cm^{-3}) to better illustrate the variability along the flight path.

ACPD
11, 30665–30718, 2011

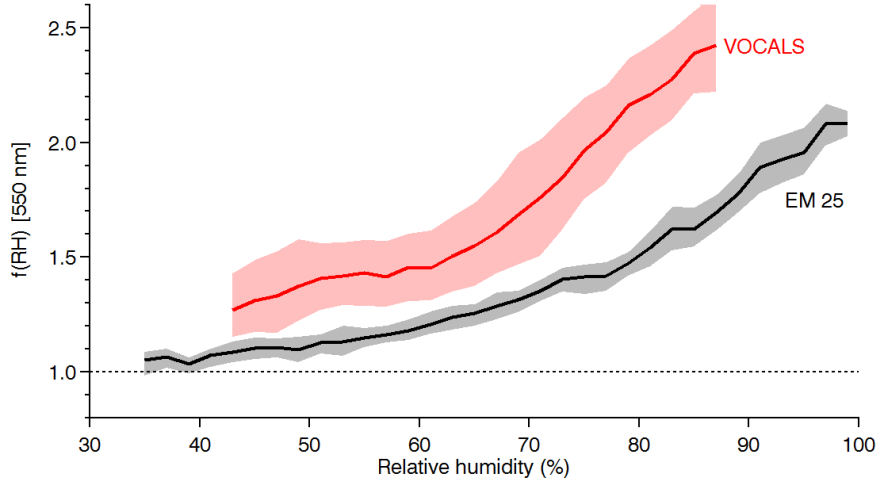

Fig. 8. Campaign-averaged ratios of humidified-to-dry corrected light scattering coefficients for 550 nm as a function of relative humidity during the EM25 (London, black) and VOCALS (south-eastern Pacific, red) campaigns. Solid lines indicate the median values and the shaded region shows the inter-quartile range. Dashed line shows no change in light scattering upon humidification.

ACPD
11, 30665–30718, 2011

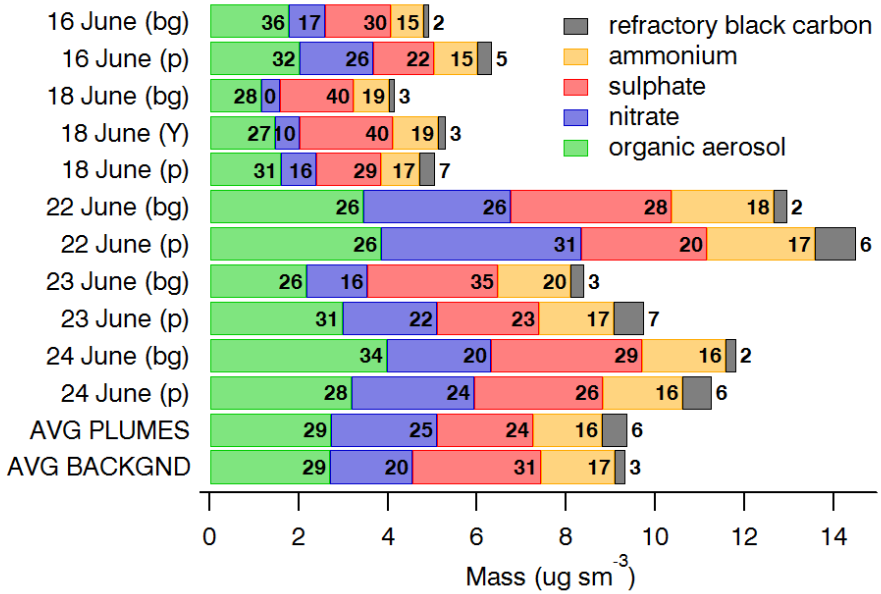

Fig. 9. Mass concentrations of AMS- and SP2-measured species averaged over London plume (p) intercepts and 'background' (bg) regions for each flight and the campaign-averaged values for all plume and background samples. The average surrounding point Y depicted in Fig. 10 for the 18 June flight is also shown. Black numbers give the mass fraction (%) of each species to the corresponding total sub-micron mass.

ACPD
11, 30665–30718, 2011

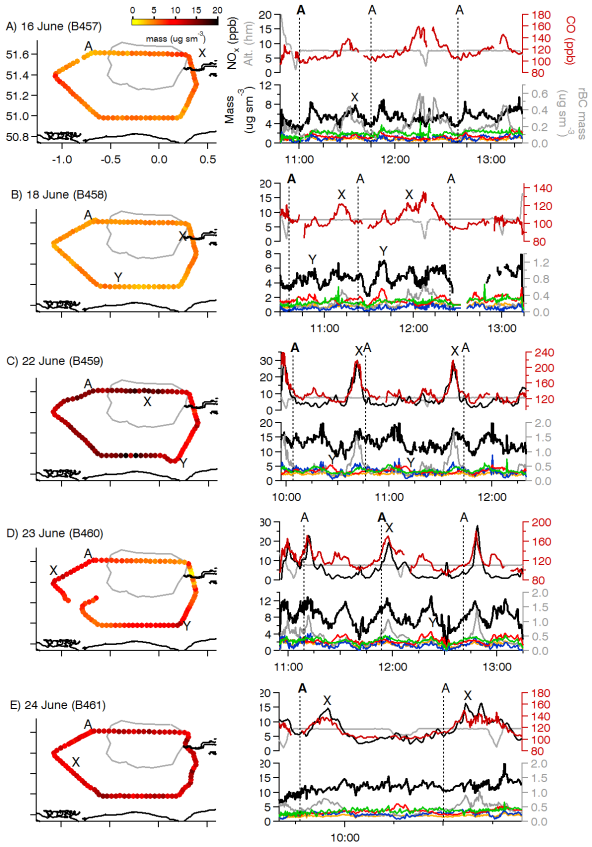

Fig. 10. Examples of aerosol sub-micron mass concentrations measured during a single circuit around London for each flight. Also shown are time series for altitude (grey), nitrogen oxides (black), carbon monoxide (red), aerosol sulphate (red), nitrate (blue), organics (green), ammonium (orange), and refractory black carbon (grey) measured by the AMS and SP2. The time series are restricted to periods when the aircraft was flying circuits around London. Points "A", the location of the London plume ("X") and other points of interest ("Y") are marked for the flight track and in the time series.

ACPD
11, 30665–30718, 2011

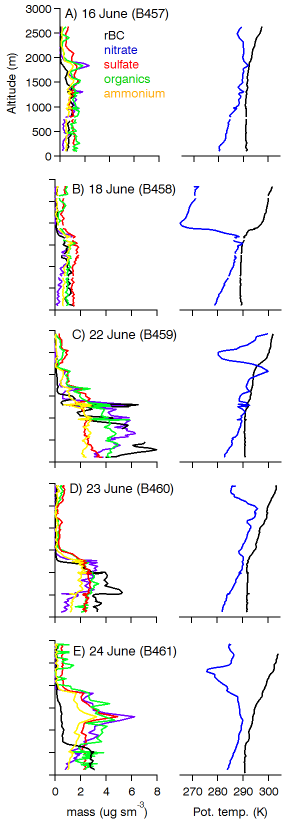

Fig. 11. Altitude profiles in the vicinity of Northolt airfield (Fig. 1) for (left) sub-micron aerosol mass concentrations over London and (right) potential temperature (black) and potential dew point temperature (blue). Refractory black carbon (rBC) was measured by the SP2 and organics, nitrate, sulphate and ammonium were measured by the AMS. rBC mass concentrations were multiplied by five to appear on the same scale as the AMS species. The horizontal grey line shows the altitude of the around London circuits. All axes are to identical scales.

ACPD
11, 30665–30718, 2011

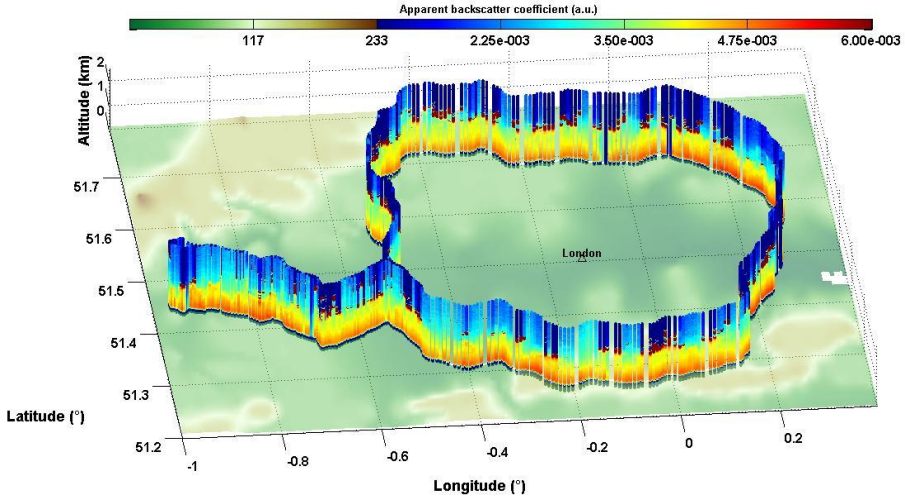

Fig. 12. Apparent lidar backscatter coefficient at 355 nm measured around the M25 motorway on the 16 June.

ACPD
11, 30665–30718, 2011

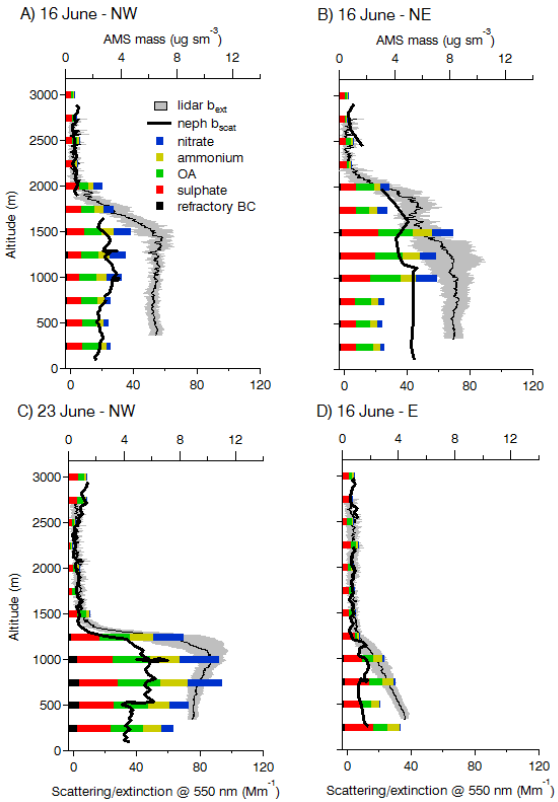

Fig. 13. Aircraft measured aerosol composition (averaged over 250 m thick altitude bins, coloured bars) and scattering coefficients (thick black lines) for individual profile segments flown to the **(a)** northwest and **(b)** northeast of central London on 16 June and **(c)** northwest and **(d)** east of central London on 23 June. Average light extinction coefficients (thin black lines) retrieved from van-based lidar measurements in the vicinity of the aircraft profiles and their variance expressed as a root mean square (shaded grey region) are also shown.

ACPD
11, 30665–30718, 2011